Trends in Analytical Chemistry 163 (2023) 117064

Contents lists available at ScienceDirect

Trends in Analytical Chemistry

journal homepage: www.elsevier.com/locate/trac

Affinity bioelectroanalysis in cellular-level biomarker driven modern precision cancer diagnosis

Susana Campuzano*, Maria Gamella, María Pedrero, José M. Pingarrón**

Departamento de Química Analítica, Facultad de CC. Químicas, Universidad Complutense de Madrid, 28040, Madrid, Spain

ARTICLE INFO

Article history:
Received 23 January 2023
Received in revised form
17 March 2023
Accepted 14 April 2023
Available online 15 April 2023

Keywords:
Affinity biosensing
Electrochemical
Cells
Secretomes
Exosomes
Cancer
Precision diagnosis

ABSTRACT

The increasingly prominent role played by precision, equitable and sustainable diagnosis, particularly of prevalent and highly heterogeneous diseases, based on the determination and characterization of biomarkers of cellular origin in liquid biopsy, such as whole cells, their secretomes and the exosomes they release, is unquestionable. Electrochemical biosensing and biosensors, mainly those involving affinity reactions, have emerged in recent years as competitive analytical alternatives to address these challenging targets versus other existing strategies in terms of simplicity, cost and compatibility with multiplexed or multi-omics point-of-care determinations. This review article aims to put on the table in a concise, accurate and updated way the fundamentals, versatility and opportunities provided by state-of-the-art electrochemical biosensing (2018–2022) for the determination of these cellular-derived biomarkers. A more critical and personal view of the challenges to be faced in the shorter term and where future research and advances are expected to go is also given.

1. Introduction

Precision medicine, a current strategic approach for patient management, sees patients as individuals rather than as part of the wider demographic [1]. This approach is driven by the identification, validation, and determination of molecular signatures of multi-omic profiling biomarkers and is becoming increasingly important in multiple highly prevalent and heterogeneous diseases, such as oncological and neurodegenerative ones, which involve many genetic disorders and unique molecular profiles.

It is important to note that precision medicine has been greatly boosted by liquid biopsy research. Liquid biopsy, the detection of circulating target molecules in body fluids, comprising, among others, circulating tumor cells (CTCs), circulating tumor DNA (ctDNA), RNA (mRNA and microRNA) and microvesicles [2], which are considered to have diagnostic, prognostic or predictive value, is a strategy that has gained and continues to gain acceptance rapidly as a method to contribute to real-time diagnosis, monitoring, staging and precision therapy particularly in spatially and temporally dynamic diseases such as cancer. Liquid biopsy offers advantages over solid (or tissue) biopsy in the earlier detection of cancer (or its possible recurrence) before the development of tumors and/or lesions large enough to be detected by subsequent biopsy. In addition, it can be taken frequently with fewer side effects and lower medical costs and reflects the circulating disease in real time by collecting information on the spatial and temporal heterogeneity of the tumor, thus allowing for improved therapeutic efficacy [3]. All this has led liquid biopsy is considered the ideal complementary tool to tissue biopsy, which is still considered necessary to establish certain subtypes of cancer, such as lung and breast cancer. However, despite the tremendous potential of liquid biopsy, its adoption in clinical practice is being slower than desirable. This may be justified by: (i) the demands in terms of required sensitivity and selectivity; (ii) the barriers to widespread implementation, such as cost, resource use and feasibility; (iii) the lack of standardized methodologies for collection and validation required for routine clinical implementation; and iv) the procurement of regulatory approvals from national and international agencies. Nowadays there is a firm conviction that the exploitation of liquid biopsy for the benefit of a cutting-edge precision medicine, with an increasing impact on research and healthcare, mainly for oncological patients, and egalitarian healthcare, has a long way to go that can be cut short by the development of disruptive technologies

* Corresponding author.
** Corresponding author.
E-mail addresses: susanacr@quim.ucm.es (S. Campuzano), pingarro@quim.ucm.es (J.M. Pingarrón).

https://doi.org/10.1016/j.trac.2023.117064

enabling the identification, validation and determination of new biomarkers at the multiplexed and/or multi-omics level in an affordable and sustainable decentralized manner. In this field, electrochemical biosensing and biosensors have much to say and offer, together with the application of machine learning-based approaches to optimize the interpretation of the obtained results [4].

The interest in the development of electrochemical affinity sensors to carry out the determination of cancer biomarkers has grown exponentially until 2018−19 (WoS source), stabilizing since then. Between 2019 and 2022 around 500 articles were published on this topic: 18.5% in 2019, 27.5% in 2020, 25% in 2021 and 29% in 2022. Moreover, this topic has received 22 170 citations between 2019 and 2022, 18% in 2019, 22.5% in 2020, 29% in 2021 and 30.5% in 2022, which confirms the current high interest of the topic which, in addition, has remained constant for the last four years.

Knowing firsthand the important and unique assets of electrochemical biosensing technology in precision medicine, we intend with this review to bring to scene their potential to chase cellular biomarkers, including the cells themselves, their secretomes and the exosomes they release, with which perhaps the scientific audience may be less familiar but also with much to bring to individualized diagnostics.

It is important to note that, although due to the relevance and topicality of the subject there are recent and interesting reviews devoted to electrochemical biosensors for the determination of cancer biomarkers [5,6] and some that pay particular attention to the determination of exosomes [7,8] or whole cells [9−12], to our knowledge none of them cover cellular secretomes and joint detection of cells, exosomes and secretomes with particular attention to their potential in modern precision cancer diagnosis nor delve into the unique opportunities provided by electroanalytical affinity bioassays/biosensors for this purpose.

2. Precision cancer diagnosis. Biomarkers on the crest of the wave

Until recently, treatments were designed with a “one-fits-all” approach founded on traditional phenotypic diagnoses based on symptoms and signs, which failed to achieve the expected benefits in many patients. Advances in the identification of genetic and molecular biomarker profiles, preferably using minimally invasive samples, which reflect biological alterations with prognostic or predictive value, have opened the door to a new approach, known as precision medicine, which seeks to adapt treatments (in terms of type, dose and time of application) to the attributes and/or stage of the disease of each individual, thus improving its efficacy and minimizing unnecessary adverse effects [1,13,14]. In addition, the fact that a patient can access precision treatments is a right that allows them to participate in their self-care and enjoy a longer and better-quality life and, in the face of society, it means a more rational and economical use of the resources.

Although precision medicine is already allowing higher survival rates in cancer patients with the worst prognosis [15] and also incurring very promising results in other prevalent diseases such as neurodegenerative and autoimmune diseases, its implementation in egalitarian health care is conditioned by the deployment of innovative technologies, at an affordable cost, which allows progress in research and in the identification, validation and determination of new biomarkers.

On the other hand, the COVID-19 pandemic has revealed as never before the deficiencies of the health systems in the diagnosis and treatment of cancer, neurological diseases, and viral infections, among others, as well as the gaps in their research. A recent report by a group of experts warns that Europe may face a “cancer epidemic” in the next decade [14,16].

Against the backdrop of the pandemic, Brexit, the Russian invasion of Ukraine and the economic downturn, it is imperative to prioritize a research environment that plays a transformative role in improving prevention, screening and early detection of these diseases to reduce the number of people who develop them and allow those who do have access to more affordable, higher quality and more equitable care, ensuring a longer and higher quality life. The time has come to reimagine the investigation of these diseases and their detection and clinical management and to move towards biomarker-based approaches. This will undoubtedly be driven by the development of disruptive technologies with the potential to promote precision medicine and biomarker-based research, able to function even independently of healthcare institutions (e-health) and to contribute to sustainable development.

Taking into account the growing relevance that they are gaining for early diagnosis and for the application of therapies with improved efficiency and with fewer side effects, precision medicine currently pursues, in addition to the determination of circulating biomarkers of protein and genetic nature, the detection and determination of other more challenging biomarkers at the cellular level such as the whole cells themselves [9,11,12,17], exosomes that they secrete [7,8,18] and their secretomes.

We should note briefly here also the role that three-dimensional (3D) tumor models, such as spheroids, organoids, biopolymer scaffolds, tumor-on-a-chip and organ-on-a-chip models, more reflective than the traditional two-dimensional (2D) cell culture models of human tumor-like features, including hypoxic regions and gradient distribution of chemical/biological factors, have to provide basic and translational research to advance and widen the understanding of precision medicine [19−23]. Organoids, considered an intermediate model in precision medicine, are t3D *in vitro* culture platforms constructed from self-organizing stem cells which can almost accurately recapitulate tumor biology and microenvironment “in a dish,” surpassing the established 2D culture cell models, usually limited to mimicking the real 3D physiological conditions, cell heterogeneity, cell to cell interaction, and extracellular matrix (ECM) present in living tissues [22]. Moreover, organoids are not so expensive and time-consuming as patient-derived tumor xenografts. Organoids are crucial tools to model organ or tissue development and human diseases and to study fundamental processes such as hypoxia, oncogenesis and metastasis and can be stored as “living biobanks” [19]. In addition, multiple 3D organoids can relate to a vascular network to develop an “organ-on-a-chip” (OoC), a microsystem with chambers at the macro scale where living cells can grow and are continuously perfused. These systems mimic the physiological environment of organs by introducing key parameters such as concentration gradients, mechanical compression, fluid shear-force, and by allowing organized cell patterning, having been developed for several organs and tissues [22].

3. Empowered affinity electrochemical biosensing

Electrochemical bioplatforms, with a roadmap demonstrating the successful determination of a large panoply of relevant clinical biomarkers, possess unique features, such as simplicity, high sensitivity and selectivity, cost-effectiveness, rapid response, ability to be highly customizable and adaptable, inherent miniaturization, scalable manufacturing, use of low power consumption instrumentation, easy implementation on different types of substrates and integration into portable devices, versatility to obtain multiomic biomarker profiles on complex, poorly treated samples, and the reduction of required assay times and sample quantities compared to other state-of-the-art technologies available for the

determination of proteomic, transcriptomic and epigenetic biomarkers. All these singularities position electrochemical bioplatforms as suitable alternatives to address the challenges posed by the implementation of precision medicine and avoid the terrible consequences of unexpected pandemics like Covid-19 [1,24].

The advances in bioelectroanalytical methods with improved performance have gone hand in hand with:

- The development of new electrochemical substrates exhibiting advantages for point-of-care (POC) applications [24]: disposable screen-printed electrodes (SPEs) or field-effect transistors (FETs) and more recently paper, plastic, textile, polymeric, temporary tattoo or bioinspired superwettable substrates.
- The production and application of new bioreceptors obtained by innovative technologies (HaloTag and phage-display), overcoming the limited commercial availability and the problems that conventional strategies for their production/purification/storage may present.
- The use of ratiometric methods based on the measurement of the relationship between two independent signals (generally with opposite tendencies and only one dependent on the target response) instead of the absolute value of a single signal. These methods have shown to provide less conditioned responses to variations in the electrode fabrication/modification, presence of interferents, or changes in environmental conditions, thus allowing determinations with improved precision, reproducibility, selectivity, and reliability [25].
- The rational design of surfaces with attractive chemistries (diazonium salts [26], monolayers of multicomponent thiols [27]) or electrode modifiers (transient polymers) [28] to impart unique biofunctionalization and/or antifouling properties [29].
- The exploitation of the intrinsic merits of biological compatibility, excellent physicochemical features, and unique catalytic ability of individual or hybrid artificial or biological nanomaterials as electrode modifiers, advanced labels, signal element transporters and/or artificial enzymes [30].
- The incipient exploration of characteristic nucleic acid probes (poly(A) or "Y-shaped" probes) and multifunctional and/or multimeric bioreceptors (mainly aptamers and peptides).
- The use of amplification strategies easily implementable in devices at the POC based on: i) Isothermal amplification of nucleic acids (hybridization chain reaction, HCR, rolling circle amplification, RCA); ii) nucleic acid and/or probe recycling strategies (which overcome the limitations imposed by the stoichiometry of the reaction); and iii) novel bioassay formats combined with bioreceptors carrying multiple signaling elements.
- The coupling of new molecular tools such as CRISPR-Cas technology [31–33].
- The application of electrochemiluminescence (ECL) in the detection step. This technique, in which electrogenerated chemiluminescence signals are usually obtained from the excited states of a luminophore generated at the electrode surface during the electrochemical reaction, exhibits interesting intrinsic properties including low background noise, high sensitivity, excellent controllability, wide range of detection, low cost, ease of use and portability [34,35].

It is this empowerment in properties and opportunities that has allowed electroanalytical bioplatforms to incur and demonstrate unthinkable pioneering applications to assist in the precision medicine of prevalent diseases, mainly cancer, but also autoimmune and neurodegenerative diseases [24]. The following sections critically discuss the foundations, noting merits and potential applications exhibited by affinity-based electrochemical biosensors/biosensing strategies reported in the last 5 years for the determination of cellular secretomes, whole cells and derived exosomes. Strategies using ingenious designs and that have been confronted with real patients' samples are prioritized. Conclusions assessing the imminent challenges ahead and offering an outlook on the field are also given.

4. Cutting-edge electrochemical affinity biosensing in cancer-related cellular biomarkers

4.1. Whole cells

Tumor heterogeneity poses a great challenge for cancer diagnosis, as the molecular profile varies from site to site with different disease progression [36]. In this context, circulating tumor cells (CTCs), viable cancer cells that detach from a primary tumor and circulate in the peripheral blood to form secondary tumors, acting as the cellular origin of metastasis (the major cause of cancer-associated mortality) and relapse [37,38], are considered a potential alternative to surpass the flaws and limitations found in performing conventional needle biopsies (sometimes difficult to obtain due to the remote location of the tumor, with risk of tumor seeding and limited sampling opportunities [39,40]). There is increasing evidence that quantification and characterization of CTCs play a crucial role in early diagnosis, assessment of cancer spread, prediction of patient prognosis and evaluation of therapeutic treatments. However, the isolation, detection, and classification of CTCs in blood face to huge challenges due to their extremely low abundance (1–10 CTCs per mL in the early-stage cancer patients [41]) among a large number (10 million leukocytes and 5 billion erythrocytes in 1 mL of blood) [42,43]. Also noteworthy is the potential of cancer stem cells (CSCs), a subpopulation of tumor cells that can drive tumor initiation and can cause relapses, in targeted precision therapies [44,45].

Table 1 summarizes the rationale and the most relevant characteristics of representative electrochemical affinity biosensors and biosensing strategies reported since 2018 for the determination of whole tumor cells.

In general, these methods ingeniously combine amplification strategies (isothermal of nucleic acids or use biological or artificial nanomaterials as electrode modifiers, signaling elements or their carriers and nanozymes) with different bioassay formats (direct, sandwich or displacement) and affinity bioreceptors (aptamers, antibodies, lectins and peptides) to achieve the high sensitivity and selectivity required for the determination of these especially challenging targets. Some particularly noteworthy advances include the exploitation of nanomotors, paper substrates, positively charged mesoporous silica nanoparticles (PMSN) as biogates, and probes involving quantum dots (QDs), Ag nanomaterials, p-sulfonatocalix [4]-arene (pSC_4) and ssDNA-dAb.

As it can be seen in Table 1, the selective determination of target cells is performed using bioreceptors capable of specifically recognizing the target cell or any of the molecules expressed on its surface (EpCAM, N-glycan, PTK7, NCL, MUC1, CD44, HER2 and amino acid residues) while transduction is made by conventional electrochemical techniques, although ECL has also incurred. Regarding the type of electrodes, most of the highlighted methods use conventional electrodes (GCE, AuE or ITO) and only a few screen-printed electrodes (SPEs). Importantly, although several methods achieve very competitive detection limits (below 10 cells), so far most of them have been applied to the analysis of supplemented human biological fluids (blood, serum, and plasma) and only one to actual clinical samples [38]. However, it is important to note that some of these methods exhibit particularly relevant capabilities including the possibility of determining, in addition to target cells, the inhibitors of N-glycan expression and the

Table 1
Electrochemical affinity biosensors/bioassays reported (2018-) for targeting whole cells.

Electrode	Rationale	Target biomarker	Target cell	Electrochemical transduction	Analytical characteristics	Application	Ref.
GCE	Nonenzymatic amperometric bioassay for determination of CTCs and N-glycan dynamical expression on their surface involving aptamer-Fe_3O_4@SiO_2−NH_2 NPs as biocaptors and Con A-Pd@Au NPs as nanolabels	EpCAM (aptamer), N-glycan (ConA)	MCF-7	Chronoamperometry (H_2O_2) "Signal on"	LR: 100−1 × 10^6 cells mL^{-1} LOD: 30 cells mL^{-1}	Cells treated with inhibitors of N-glycan and O-glycan expression	[41]
ITO	Amplification-free, label-free, and enzyme-free homogeneous electrochemical biosensing strategy based on the target-induced displacement reaction using aptamer-capped PMSN with $[Fe(CN)_6]^{3-}$ entrapped as biogates	SK-BR-3	SK-BR-3	DPV ($[Fe(CN)_6]^{3-}$) "Signal on"	LR: 40−1.7 × 10^6 cells mL^{-1} LOD: 13 cell mL^{-1}	–	[46]
AuE	Label-free aptasensor based on the use of a thiolated DNA aptamer	PTK7	Jurkat cells	EIS ($[Fe(CN)_6]^{3-/4-}$) "Signal on"	LOD: 105 ± 10 cells mL^{-1}	–	[47]
AuE	Aptasensor based on AuE nanostructured with DNA NTHs, and aptamer-MIL-101(Fe)@AuNPs nanoprobes decorated numerous hemin/G-quadruplex DNAzyme and natural HRP using multibranched HCR	HepG2	HepG2	DPV (hemin/H_2O_2/HQ) "Signal on"	LR: 1.0 × 10^2−1.0 × 10^7 LOD: 5 cells mL^{-1}	Spiked human blood	[48]
AuE	Signaling probe displacement electrochemical aptasensor prepared by immobilizing a thiolated NCL specific aptamer to a IL/HApNR-AuNP/AuE and using c-DNA@AgNPs as signaling nanoprobes	NCL	MCF-7	DPV (AgNPs) "Signal off"	LR: 10−10^6 cells mL^{-1} LOD: 8 ± 2 cells mL^{-1}	Spiked human serum	[49]
Au SPE	Label-free electrochemical platform based on DNA NTH assembled onto Au SPE, multifunctional nanoprobes fabricated through a DNA primer probe, FAM-functionalized aptamer and HRP immobilized on the surfaces of PtNPs and RCA directed DNAzyme strategy	HepG2	HepG2	DPV (hemin/H_2O_2/HQ) "Signal off"	LR: 10−1 × 10^6 cells mL^{-1} LOD: 3 cells mL^{-1}	Spiked human blood	[50]
Au SPE	Label-free electrochemical platform based on aptamer-DNA NTH assembled onto Au SPE and hybrid nanoprobes of Pd−Pt nanocages labeled with cDNA, hemin/G-quadruplex DNAzyme and HRP	HepG2	HepG2	DPV (hemin/H_2O_2/HQ) "Signal off"	LOD: 5 cells mL^{-1}	Spiked human blood and feasibility to release the captured cells from substrate without any damage	[37]
GCE	Aptasensor fabricated using rGO/AuNPs-GCE and aptamer-CuO NPs as nanoprobes	MUC1	MCF-7	DPV (H_2O_2) "Signal on"	LR: 50−7 × 10^3 cells mL^{-1} LOD: 27 cells mL^{-1}	Spiked human serum	[51]
–	Electrospun PLGA nanofibers-deposited Ni micropillars-based 3D sensor to capture the target cells and dAb-QDs as nanoprobes	EpCAM	MCF-7	DPV (Cd^{2+}) "Signal on"	LR: 10^1−10^5 cells mL^{-1} LOD: 8 cells mL^{-1}	Spiked human plasma and blood samples from gastric and lung cancer patients	[38]
GCE	Aptamer-MnO_2-PEI/Ni/Au self-propelled nanomotors to isolate the target cells and their determination at an aptamer/PEDOT-AuNPs/GCE	HL-60	HL-60	EIS ($[Fe(CN)_6]^{3-/4-}$) "Signal on"	LR: 2.5 × 10^1−5 × 10^5 cells mL^{-1} LOD: 250 cells mL^{-1}	–	[52]
AuE	Immunosensor based on the use of a cAb-Prot G-AuNPs/AB-AuE and dAb-Pt@AgNFs as nanocarriers	EpCAM	MCF-7	DPV (H_2O_2) "Signal on"	LR: 20−1 × 10^6 cells mL^{-1} LOD: 3 cells mL^{-1}	Spiked human blood	[39]
GCE	3D GF/Au NCs + MWCNTs/cAb/GCE and ssDNA-dAb as probes	ER	MCF-7	SWV ($[Fe(CN)_6]^{3-/4-}$) "Signal off"	LR: 1.0 × 10^2−1.0 × 10^6 cells mL^{-1} LOD: 80 cells mL^{-1}	–	[53]
CCE	Aptamer-MWCNT-PGA/GCE and aptamer-AgNPs	MUC1	MCF-7	DPV (AgNPs) "Signal on"	LR: 1.0 × 10^2−1.0 × 10^7 cells mL^{-1} LOD: 25 cells mL^{-1}	Spiked human serum	[54]
AuE	A binding-induced DCHA electrochemical biosensor involving a specific aptamer	MUC1	A549	DPV (AP/α-NP) "Signal on"	LR: 500−100 000 cells mL^{-1} LOD: 325 cells mL^{-1}	Spiked human blood	[55]
AuE	Peptide-modified AuE in connection with CB[8] and FF-AuNPs	CD44	CD44-positive BCSCs	LSV (AgNPs) "Signal on"	LR: 10−10^6 cells mL^{-1} LOD: 8 cells mL^{-1}	–	[56]
AuE	AuE modified with a specific thiolated aptamer and pSC_4−AgNPs as universal nanoprobes	HepG2	HepG2	LSV (AgNPs) "Signal on"	LR: 5−2.5 × 10^5 cells LOD: 5 cells	–	[57]
ITO	ITO electrode modified with a NCL-specific aptamer and using Ab_{MUC1}-DNA-AgNCs as detector nanoprobes	NCL and MUC1	MCF-7	LSV (AgNCs) "Signal on"	LR: 10−5 × 10^5 cells LOD: 3 cells	–	[36]
AuE	TSA-based electrochemical aptasensor involving an aptamer-AuE, Pt NPs@HRP@aptamer composite as catalytic probe and ICP@Tyr as electroactive signal tag	NCL	HeLa	DPV (H_2O_2/Fc) "Signal on"	LR: 2−2 × 10^4 cells mL^{-1} LOD: 2 cells mL^{-1}	Spiked white blood cells	[58]
GCE	Green electrochemical strategy involving GCE/GO/PANI/GA/Con A aptamer-DNA concatamer-CdTe QDs and electrochemical detection at GCE/GR-PDDA/L-Cys	K562	K562	ASV (Cd^{2+}) "Signal on"	LR: 1.0 × 10^2−1.0 × 10^7 cells mL^{-1} LOD: 60 cells mL^{-1}	–	[59]
GCE		EpCAM				Spiked human serum	[42]

Table 1 (*continued*)

Electrode	Rationale	Target biomarker	Target cell	Electrochemical transduction	Analytical characteristics	Application	Ref.
	Label-free aptasensor based on aptamer-AuNSs-GCE and DPEE		CCRF-CEM	Amperometry (AA) "Signal off"	LR: 5–1 × 10^5 cells mL^{-1} LOD: 5 cells mL^{-1}		
SPCE	Sandwich immunoassay implemented on the surface of MBs enzymatically labeled with AP	HER2	SK-BR-3	LSV (3-IP/$AgNO_3$) "Signal on"	LOD: 3 cells mL^{-1}	–	[60]
- ECL detection -							
AuE	Stackable lab-on-paper device with all-in-one Au Electrode with a detection zone functionalized with CZRs, GQDs and DHAP labeled with Ag_2Se QDs	MCF-7	MCF-7	PEC "Signal off"	LR: 5.0 × 10^2–5.0 × 10^6 cells mL^{-1} LOD: 198 cells mL^{-1}	Spiked human serum	[61]
GCE	HCNT-based immunosensor involving the use of cAb-MNs and aptamer-Cu_2O NPs	EpCAM	MCF-7	PEC "Signal off"	LR: 3–3000 cell mL^{-1} LOD: 1 cell mL^{-1}	Spiked human blood	[43]

AA: ascorbic acid; AuNSs: gold nanostars; AB: acetylene black; AgNCs: silver nanoclusters; AP: alkaline phosphatase; ASV: anodic stripping voltammetry; AuNP: gold nanoparticle; Au NCs: Au nanocages; BCSCs: breast cancer stem cells; CB[8]: curbit[n]uril with eight glycoluril units; cDNA: complementary DNA; Con A: concanavalin A; CZRs: ZnO nanorods; Cu_2O NPs: Cu_2O nanoparticles; 3D GF: 3D graphene; DCHA: dual catalytic hairpin assembly; DHAP: DNA hairpin-based aptamer probe; DPEE: direct plasmon-enhanced electrochemistry; DPV: differential pulse voltammetry; EIS: electrochemical impedance spectroscopy; ER: estrogen receptor; FAM: carboxyfluorescein; Fc: ferrocene; FF: diphenylalanine; GA: glutaraldehyde; GO: graphene oxide; GQDs: graphene quantum dots; GR: graphene; HApNR: hydroxyapatite nanorod; HCNT: hexagonal carbon nitride tube; HER2: human epidermal growth factor receptor 2; ICPs@Tyr: tyramine functionalized infinite coordination polymer; IL: ionic liquid; 3-IP: 3-indoxyl phosphate; ITO: indium tin oxide; L- Cys: L-cysteine; LR: linear range; MBs: magnetic microbeads; MNs: magnetic Fe_3O_4 nanospheres; MUC1: mucin 1; MWCNT: multi-walled carbon nanotubes; LOD: detection limit; LR: linear range; LSV: linear sweep voltammetry; NCL: nucleolin; NFs: nanoflowers; α-NP: α-naphthyl phosphate; NTH: nanotetrahedron; PANI: polyaniline; PDDA: poly diallyldimethylammonium chloride; PEDOT: poly(3,4-ethylene dioxythiophene); PGA: poly(glutamic acid); PLGA: poly (lactic-co-glycolic acid); PMSN: positively charged mesoporous silica nanoparticles; pSC_4: p-sulfonatocalix [4]-arene; PTK7: protein tyrosine kinase-7; Prot G: protein G; QDs: quantum dots; rGO: reduced graphene oxide; SPCE: screen-printed carbon electrode; SPE: screen-printed electrodes; SWV: square wave voltammetry; TSA: tyramide signal amplification.

possibility to release the captured cells without compromising their viability for further characterization.

Delving into the rationale and potential of some particular methods, the strategy reported by Liu et al. for the determination of MCF-7 cells and the N-glycan dynamical expression on their surface can be highlighted. The method used as capture and detection bioreceptors an EpCAM-specific aptamer and a lectin (Concanavalin A, Con A) capable of recognizing N-glycan [41]. In fact, the strategy combined the use of aptamer-Fe_3O_4@SiO_2–NH_2 NPs as biocaptors and Con A-Pd@Au NPs as nanolabels. Chronoamperometric transduction assisted by the intrinsic peroxidase-like activity of Fe_3O_4@SiO_2–NH_2 NPs, allowed the sensitive and selective detection of target cells and cells treated with N-glycan inhibitors, thus offering great potential for both the early diagnosis of cancer and for revealing N-glycan-related biological processes and diseases.

Gu et al. reported a label and enzyme-free homogeneous electrochemical platform for SK-BR-3 cells using aptamer-capped positively charged mesoporous silica nanoparticles (PMSN) with electroactive probes ($[Fe(CN)_6]^{3-}$) entrapped as biogates. The rationale involved a target-induced displacement reaction, and differential pulse voltammetry (DPV) detection of the oxidation of the $[Fe(CN)_6]^{3-}$ molecules released from the opened biogates in the presence of the target cells [46].

The aptasensors developed by Zhang's group [37,48,50] exhibited the advantages provided by electrospun surface nanostructuring with DNA nanotetrahedra (NTHs) to immobilize the aptamer with the best conformation, packing density and spacing to ensure the best efficiency in the target cell biorecognition process [62]. The developed aptasensors further explored the advantages of different types of nanoprobes (MIL-101(Fe)@AuNPs, PtNPs, Pd–Pt nanocages), DNAzymes (hemin/G-quadruplex) and natural HRP and nucleic acid isothermal amplification strategies (multi-branched HCR, RCA). DPV transduction in the presence of hemin/H_2O_2/HQ was utilized for the sensitive determination of HepG2 cells (LODs: 3–5 cells mL^{-1}) and the methods were applied to the analysis of spiked human blood samples. As a representative example, Fig. 1 displays the aptasensor using dendritic structure (DS) nanoprobes from hybrid nanoprobes of Pd–Pt nanocages labeled with complementary DNA (cDNA), hemin/G-quadruplex DNAzyme and HRP. Fig. 1b) shows as the amplification was achieved by the formation of the DS nanoprobes (curve 3, nanoprobe 1 + nanoprobe 2) compared to using only the nanoprobe 1 in the absence (curve 1) and the presence (curve 2) of hemin. This strategy also demonstrated that the captured cells could be released from the substrate without damage by means of an electrochemical desorption method, which makes it possible further characterization or studies of the isolated cells [37].

Farzin et al. reported a signaling probe displacement-based electrochemical aptasensor [49] exploiting the use of a nucleolin (NCL)-specific aptamer immobilized through thiol chemistry on a AuE modified with a nanocomposite consisting of a hydroxyapatite nanorod (HApNR), an ionic liquid (IL) and AuNPs (the latter two to compensate for the low electrical conductivity of HAp). The IL/HApNR-AuNP/AuE was further conjugated to c-DNA@AgNPs as signaling nanoprobes, which were displaced and released from the AuE in the presence of the target cells leading to a decrease in the oxidation signal of AgNPs to Ag^+ measured by DPV. The use of HApNR-AuNP nanocomposite as the AuE modifier imparted an excellent biocompatibility, good conductivity and a high surface area allowing the immobilization of a large amount of aptamer. The aptasensor achieved a LOD of only (8 ± 2) MCF-7 cells mL^{-1} and was used to analyze spiked human serum samples.

An electrospun poly (lactic-co-glycolic acid) (PLGA) nanofibers-deposited Ni micropillars-based 3D sensor to efficiently capture MCF-7 cells further labeled through their surface EpCAM with dAb-QDs as nanoprobes was reported by Wu et al. [38] (Fig. 2). The authors claimed that Ni micropillars in the longitudinal direction played an important role in improving the conductivity for the electrochemical sensing and enhancing the cell capture efficiency. Moreover, the transversely aligned nanofibers could simulate the extracellular matrix to provide a favorable microenvironment for cell adhesion and physiological functions. By measuring the Cd^{2+} released in the acid dissolution of QDs using DPV the sensor allowed detecting just 8 cells mL^{-1} and, as can be seen in Fig. 2b), the quantification of cells in blood samples from gastric and lung cancer patients.

Tabrizi et al. reported an original strategy combining the use of aptamer-modified manganese oxide nanosheets-polyethyleneimine decorated with nickel/gold nanoparticles (aptamer-MnO_2-PEI/Ni/Au) self-propelled nanomotors to isolate quickly and efficiently HL-60 cells. The cells released from the nanomotors (by supplementing the solution with a synthetic

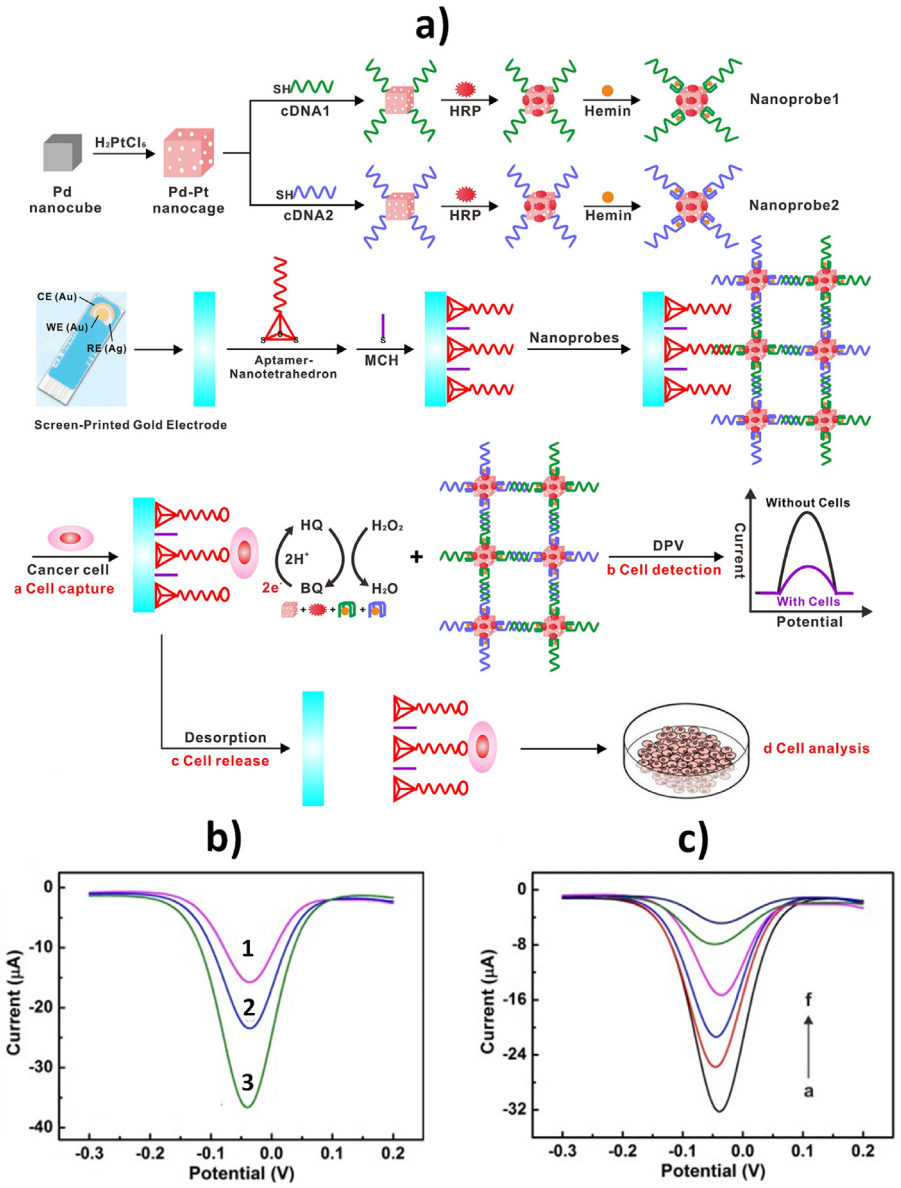

Fig. 1. a) Aptasensor for DPV detection of HepG2 cells using aptamer-DNA NTHs-AuE and hybrid nanoprobes of cDNA, hemin/G-quadruplex DNAzyme and HRP labeled Pd–Pt nanocages. b) Comparison of the DPV responses obtained using DS nanoprobes (curve 3) or only the nanoprobe 1 in the absence (curve 1) and the presence (curve 2) of hemin. c) DPV signals obtained for increasing concentrations of HepG2 cells (a–f: 10, 10^2, 10^3, 10^4, 10^5, and 10^6 cells mL^{-1}). Reprinted from Ref. [37] with permission, Copyright (2018) Elsevier.

sequence complementary to the aptamer immobilized on the nanomotors) were determined by electrochemical impedance spectroscopy (EIS) at an aptamer/gold nanoparticles-poly(3,4-ethylene dioxythiophene) modified GCE (aptamer/PEDOT-AuNPs/GCE) [52] (Fig. 3). This method, similarly to that previously reported by Sun et al. [37], allowed, in addition to quantification, other studies on the isolated cells, although in this case the authors did not evaluate their viability.

A label-free immunosensor was reported by Ref. [53] for the determination of MCF-7 cells by targeting the estrogen receptor (ER) expression using a GCE modified with 3D graphene and a hybrid of Au nanocages (Au NCs)/amino-functionalized multi-walled carbon nanotubes (MWCNT-NH_2), and DNA-labeled antibodies (ssDNA-dAb) as detector probes (Fig. 4). Combining the advantages of ssDNA-dAb and the signal amplification strategy induced by the use of the nanomaterial, this enzyme-free immunosensor allowed detecting 80 cells mL^{-1} using square wave voltammetry (SWV) in the presence of $[Fe(CN)_6]^{3-/4-}$.

Zhang et al. [57] proposed the use of AgNPs modified with pSC_4-, which can recognize and bind to various amino acid residues on the cell membrane proteins, as universal probes for the development of an electrochemical aptasensor for the determination of K562 cells (Fig. 5). The electrochemical reduction of pSC_4-AgNPs in KCl solution attributed to the reduction of AgCl back to Ag and recorded by linear sweep voltammetry (LSV) allowed the detection of as few as 5 cells.

A very sensitive tyramide (Tyr) signal amplification (TSA)-based electrochemical aptasensor involving an aptamer-AuE, PtNPs@HRP@aptamer composite, as catalytic probe, and tyramine functionalized infinite coordination polymer (ICP@Tyr), as electroactive signal tag, was reported by Zhou et al. [58] (Fig. 6). The method achieved a LOD of 2 Hela cells mL^{-1} and was used for their discrimination against white blood cells.

Zeng et al. reported a green electrochemical strategy for

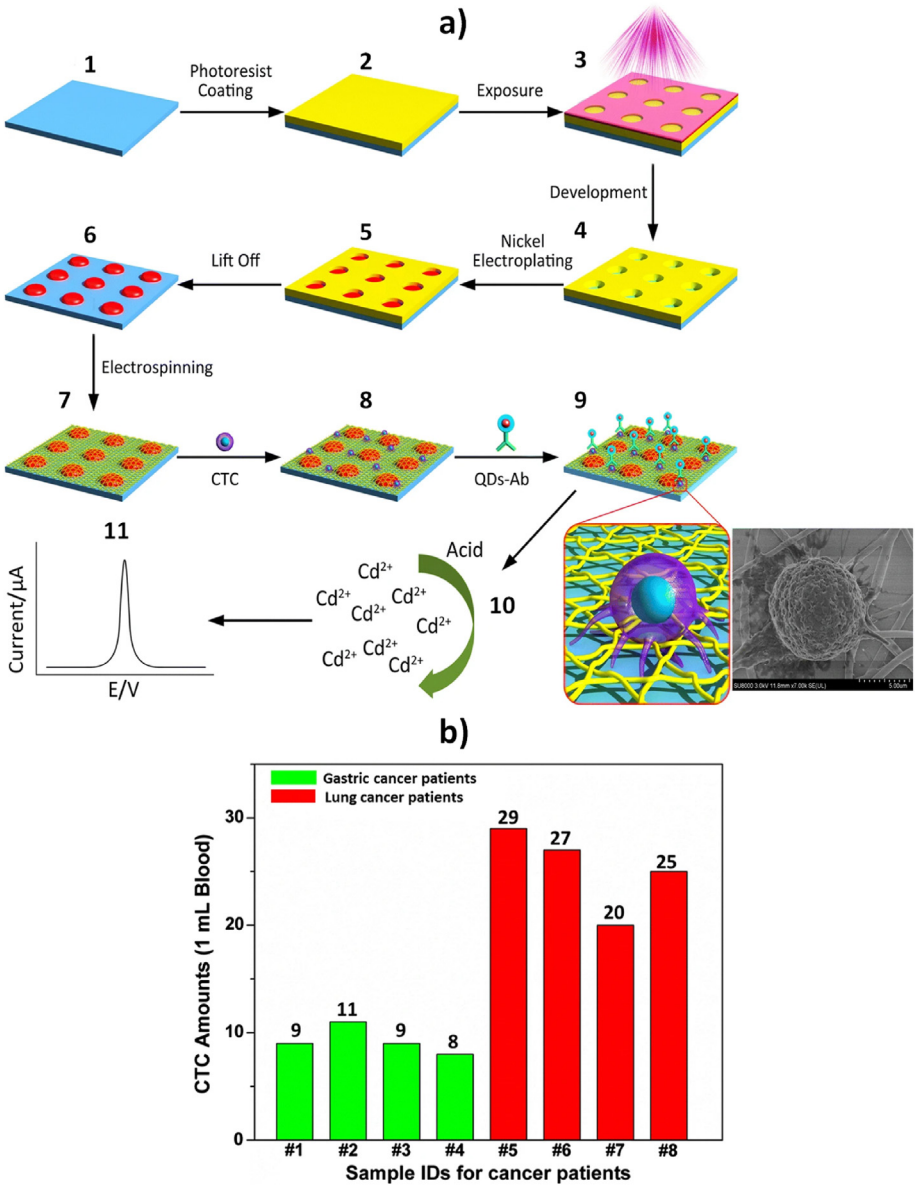

Fig. 2. a) Steps involved in the electrochemical determination of MCF-7 exploiting an electrospun PLGA nanofibers-deposited Ni micropillars-based 3D sensor and dAb-QDs as detector nanoprobes. b) Application to the quantification of the number of target cells in 1 mL of blood samples from gastric and lung cancer patients. Reprinted from Ref. [38] with permission, Copyright (2018) Springer Nature.

interrogating K562 cells involving a GCE modified with graphene oxide (GO), polyaniline (PANI), glutaraldehyde (GA) and Concanavalin A (Con A) (GCE/GO/PANI/GA/Con A), as well as aptamer-DNA concatamer-CdTe QDs probes. The electrochemical quantification of the resulting Cd^{2+} ions after acid dissolution of the QDs was made by anodic stripping voltammetry (ASV) at a GCE modified with graphene (GR), poly diallyldimethylammonium chloride (PDDA) and L-Cysteine (L-Cys) (GCE/GR-PDDA/L-Cys) [59].

Peptides have been much less used as bioreceptors than aptamers and antibodies. Nevertheless, an illustrative example is the biosensor reported by Zhao et al. [56] in connection with Cucurbit[n]uril 8 (CB[8]) and self-assembled diphenylalanine (FF) nanostructure with electrodeposited AuNPs (FF-AuNPs) for targeting CD44-positive breast cancer stem cells (BCSCs). Fig. 7 shows as only in the presence of the target cells, the cleavage by trypsin of the peptide capable of recognizing CD44 was prevented and the CB [8]-assisted immobilization of FF-AuNPs on the peptide occurred. A large electrochemical response was obtained by LSV ascribed to the oxidation of silver after silver enhancement of FF-AuNPs nanospheres.

Regarding ECL detection, strategies able to determine MCF-7 cells in spiked serum or blood samples have been reported using a stackable lab-on-paper device with all-in-one Au electrode with a detection zone functionalized with corn-like ZnO nanorods (CZRs), graphene quantum dots (GQDs) and a DNA hairpin-based aptamer probe (DHAP) labeled with Ag_2Se QDs [61] or an hexagonal carbon nitride tubes (HCNT)-based immunosensor involving the use of cAb-modified magnetic Fe_3O_4 nanospheres (MNs) and aptamer-Cu_2O NPs [43]. The latter immunosensor, whose preparation and rationale are schematized in Fig. 8, is able to detect only 1 cell mL^{-1}.

4.2. Cell-derived exosomes

Exosomes are the smallest subclass of extracellular vesicles (Φ:

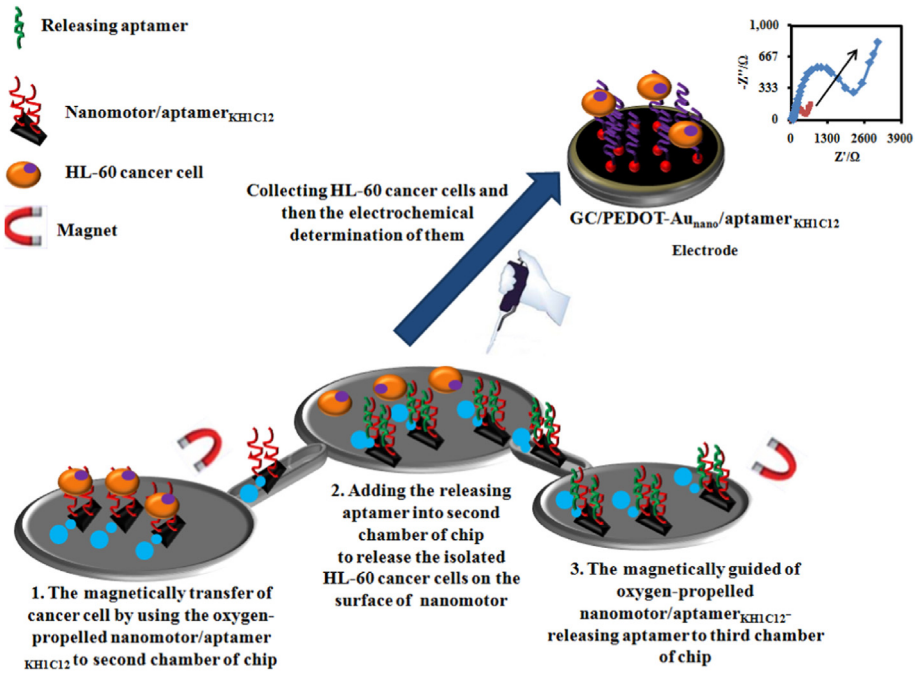

Fig. 3. Schematic diagram of the strategy developed for the isolation and impedimetric determination of HL-60 cells employing aptamer-MnO_2-PEI/Ni/Au self-propelled nanomotors and an aptamer/PEDOT-AuNPs/GCE, respectively. Reproduced from Ref. [52] with permission, Copyright (2018) Elsevier.

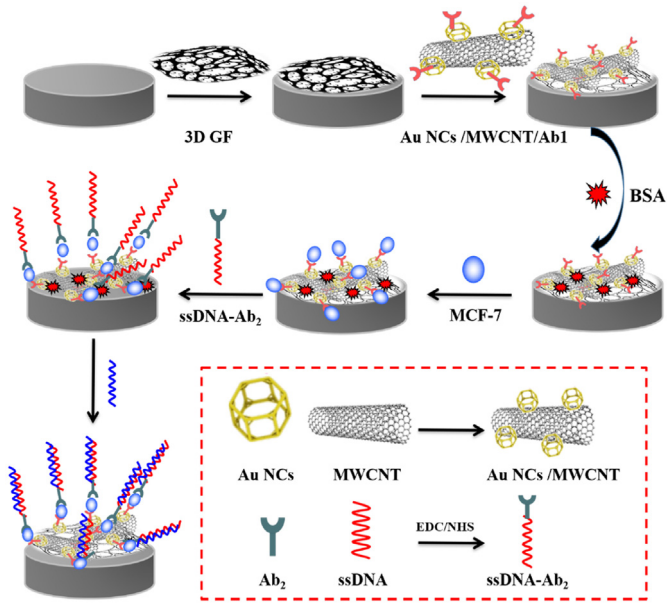

Fig. 4. Electrochemical immunosensor for the label-free voltametric determination of MCF-7 cells at a 3D GF/Au NCs + MWCNTs/cAb/GCE using ssDNA-dAb as detector probes. Reproduced from Ref. [53] with permission, Copyright (2018) Elsevier.

30–150 nm) secreted by numerous mammalian cell types. They are present in most body fluids (blood, urine, sweat, tears, saliva, breast milk, cerebrospinal fluid, semen, sputum, ascites, etc.) and tissue fluids. Their fundamental role in regulating intercellular communication and the transfer of inherent messages from progenitor to recipient cells, their involvement in various physiological and pathological processes such as metastatic niche formation, immunostimulation and cell-to-cell communication, as well as the large amount and invaluable wealth of molecular information they carry, make them highly potential candidates to contribute to the early, minimally invasive and precision diagnosis of multiple relevant pathologies [63–65]. Moreover, there is increasing evidence that the concentration and phenotypes of exosomes in biological fluids, which are more accessible than tumor samples, are closely and dynamically associated with many diseases, such as cancer, cardiovascular and neurodegenerative diseases, diabetes, and depression [35,66,67]. In fact, the number of exosomes secreted by cancer cells is at least 10 times larger than that secreted by normal cells [68]. Because of their role in tumorigenesis, invasion, metastasis and drug resistance of tumors exosomes are the so-called "hallmark of cancers" [69]. They are considered advantageous biomarkers over circulating cells because of their larger abundance and stability [7,70]. Due to their unique pathological and physiological significance, the determination and profiling of exosomes, although tremendously challenging due to their heterogeneity and the low concentration at which they are found in biological fluids [8], has gained particular importance in recent years to contribute to the timely and precision diagnosis of prevalent diseases, such as cancer. This has led to an explosion in the last 5 years in the development of innovative and enhanced affinity bioelectroanalytical tools for their determination. Their most relevant features are summarized in Table 2.

In general, by far the most used bioreceptors for the determination of exosomes are aptamers, followed by antibodies and, much less frequently by peptides which are specific to characteristic protein biomarkers expressed on their surface (mainly CD63 and EpCAM but also CD81, CD24, CD147, CD230, PD-L1, EGFR, CEA, NSE, Cyfra21-1, HER2, PSMA, MUC1, GPC1 and PS). It is important to note that some strategies have the potential to simultaneously interrogate several protein biomarkers [77] or both exosomal proteins and RNA markers [78], thus confirming the potential of bioelectroanalytical tools to address multiplexed and/or multi-omics determinations.

The strategies are based on direct or sandwich formats and to achieve the required sensitivity they used amplification strategies

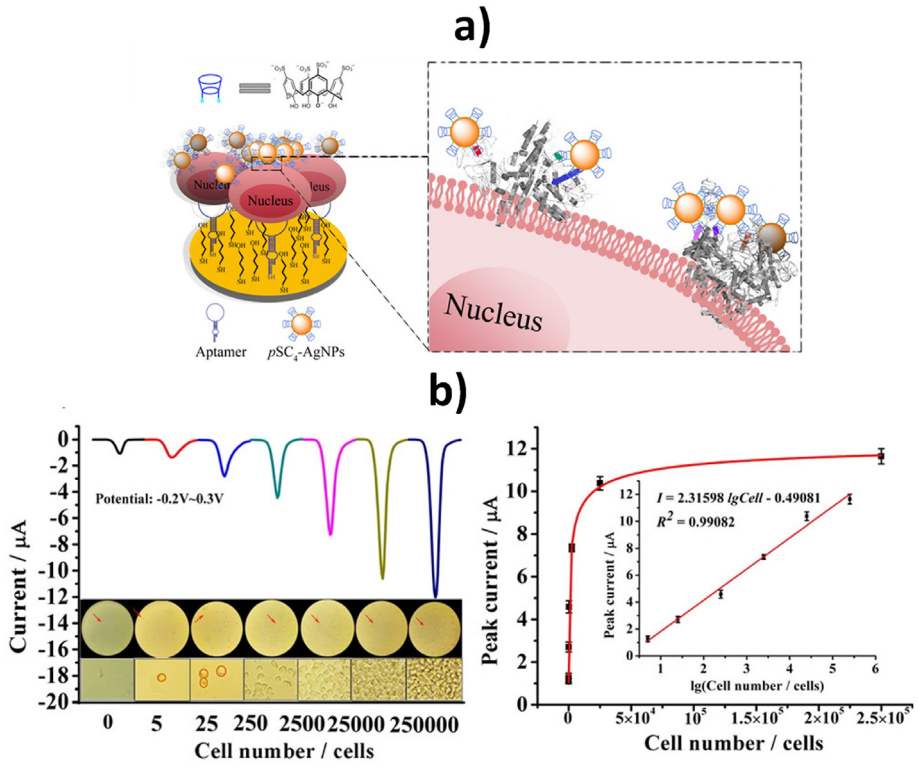

Fig. 5. a) Electrochemical aptasensor for the determination of K562 cells using pSC_4–AgNPs as universal detector probes. b) Left: LSV and images obtained for different amounts of HepG2 cells: 0, 5, 25, 2.5×10^2, 2.5×10^3, 2.5×10^4, and 2.5×10^5, Right: dependence between the peak current values and the cell amounts as well as the semi-logarithmic linear range (inset). Reprinted from Ref. [57] with permission, Copyright (2019) ACS.

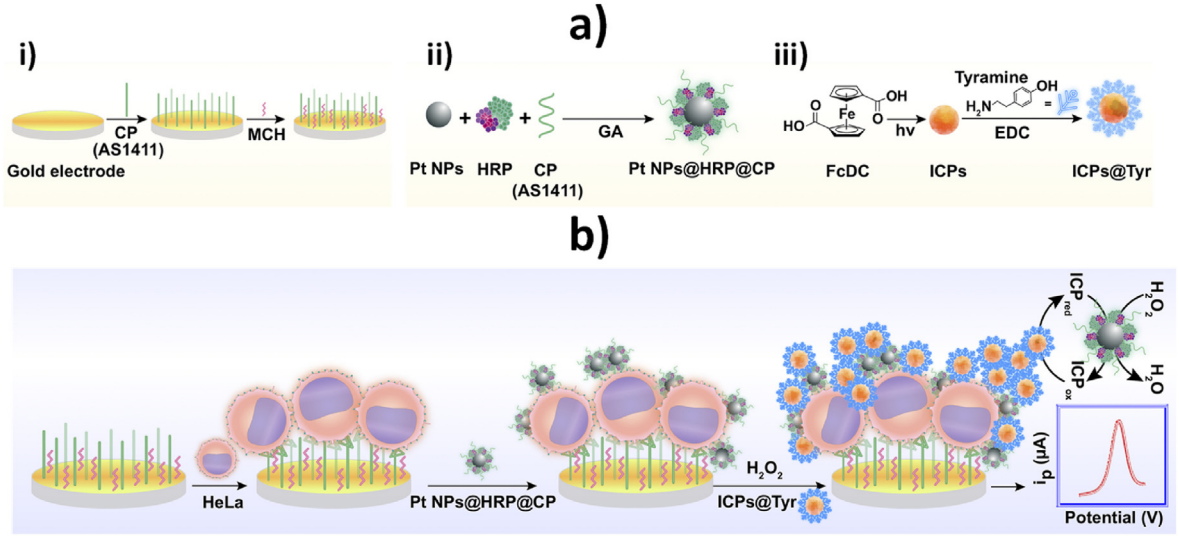

Fig. 6. a) Schematic diagrams of the fabrication of the: i) aptasensor, ii) PtNPs@HRP@aptamer and iii) ICP@Tyr. b) Rationale of the TSA-based aptasensor proposed for the sensitive determination of Hela cells. In a) CP (AS1411): Aptamer; FcDC: 1,1′-ferrocenedicarboxylic acid; GA: glutaraldehyde; MCH: mercaptohexanol. Reprinted from Ref. [58] with permission, Copyright (2019) Elsevier.

involving: i) nanomaterials, artificial or biological, as electrode modifiers, nanolabels, nanocarriers or nanozymes [72,73,89]; ii) nucleic acid isothermal amplifications (HCR and RCA both linear and nonlinear); iii) recycling of the target (Exo III- or DSN-assisted) or particular probes (CTSDR); and iv) others such as those based on DNA walking amplification. The electrochemical detection and/or biosensor implementation is usually made with conventional electrodes but also SPEs were employed.

Some of the reported methods implied the use of: i) magnetic microbeads (MBs) functionalized with appropriate bioreceptors for the selective and efficient capture of the target exosomes [69,74–76,79,81,83,90]; ii) particular chemistries such as click chemistry [61,95]; iii) paper-based substrates [89]; and iv) an enzyme-based logic system [78].

Also noteworthy is the use of metal–organic frameworks (MOFs) [89,93] or cholesterol probes [90–92] for the capture or

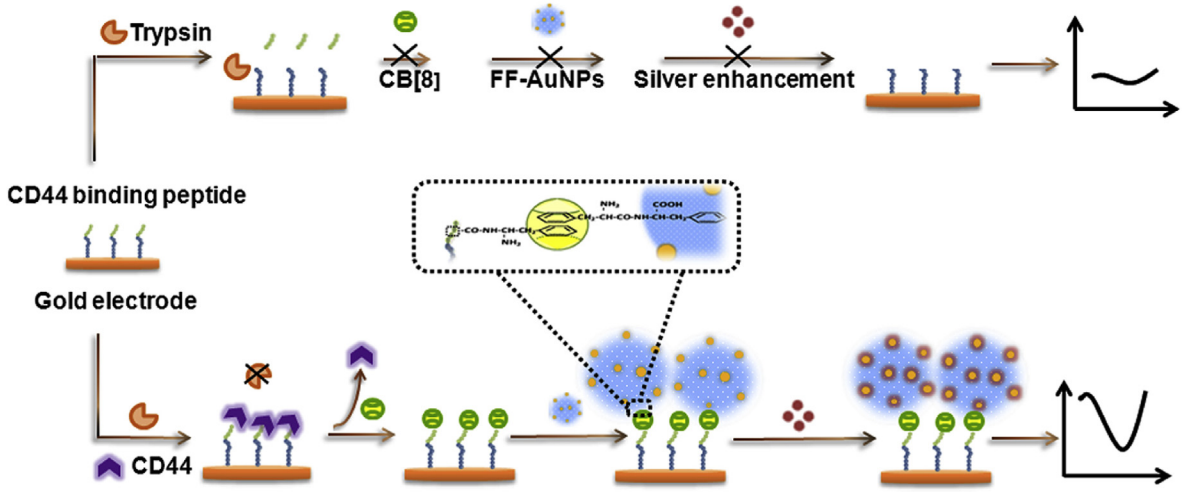

Fig. 7. Aptasensor developed to determine CD44-positive BCSCs using CB [8] and FF-AuNPs. Reproduced from Ref. [56] with permission, Copyright (2018) Springer.

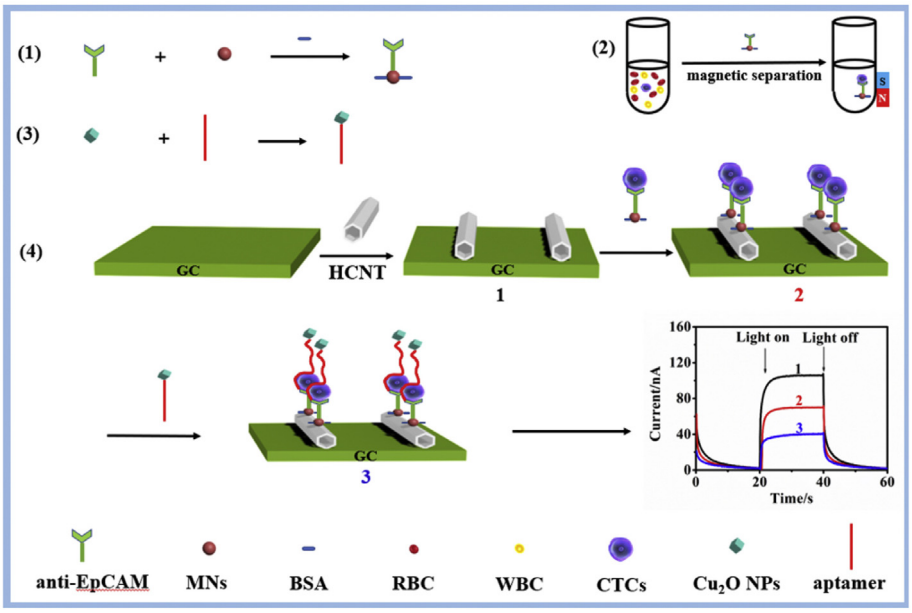

Fig. 8. ECL immunosensor using HCNT, cAb-MNs and aptamer-Cu_2O NPs as detector nanoprobes. Reproduced from Ref. [43] with permission, Copyright (2020) Elsevier.

detection of exosomes by taking advantage of their adsorption to MOFs and the interaction between cholesterol group and exosomes membrane. The development of ratiometric methodologies with improved reliability and robustness [81,92] and those using biofuel cells (BFC)-based biosensors [66] have been also reported. Although some simple and label-free methods have been developed [71,77], most are ingenious and relatively complex strategies employing mostly amperometric or voltammetric transduction, or ECL detection.

Because of its unstoppable prevalence, further propelled by the delays in diagnostics and research brought about by the COVID-19 pandemic [14], and its high mortality, the vast majority of the developed methods have been confronted for the determination of cancer cell-derived exosomes (mainly from MCF-7 but also from HeLa, PLAP, SGC7901, MDA-MB-231, MDA-MB-231, SKBR3, L02, A549, SW480, SW620, KM12C, KM12SM, KM12L4a, NCI–H1395, NCI–H226, NCI–H446, UACC-812, HL-7702, LNCaP, HepG2, HEK-293T, Colo 205, NCM-460, PC3, OVCAR, BT474, U87 and SKOV3ip) in spiked serum samples although also in samples from patients diagnosed with different types of cancer (mostly breast cancer, BC, and colorectal cancer, CRC, but also lung cancer and glioblastoma, GSM).

To show the versatility and the wide portfolio of reported methods, we discuss below the rationale and/or relevant aspects of some of the strategies summarized in Table 2.

Illustrative examples of immunosensors and immunoassay strategies that employ conventional electrochemical detection are those reported by Huang et al. [73] and Liu et al. [68].

The authors constructed an immunosensor for the determination of gastric cancer exosomes, by immobilizing a cAb_{CD63} with glutaraldehyde (GA) on a L-cysteamine-modified AuE, able to detect the exosomes captured on the surface of the cAb_{CD63}-GA- L-cysteamine-AuE, using an aptamer probe linked to a primer sequence that triggered RCA amplification and produced multiple G-quadruplex units [73]. Both the antibody used as a capture bioreceptor, and the aptamer used for detection were selective to the exosome

Table 2
Affinity biosensors/bioassays described since 2018 for the electrochemical determination of cell-derived exosomes.

Electrode	Rationale	Target biomarker	Target cell/s from which exosomes derive	Electrochemical transduction	Analytical characteristics	Application	Ref.
- Immunosensor/Immunoassays strategies -							
Au SPEs	Label-free direct immunosensor	CD81	MCF-7	DPV, EIS ($[Fe(CN)_6]^{3-/4-}$) "Signal-off"	LR: 10^2–10^9 EV mL^{-1} LOD: 77 EV mL^{-1} (EIS) and 379 EV/mL (DPV)	EVs secretion levels of hypoxic and normoxic MCF-7 cells	[71]
SPCE	Sandwich immunosensor involving cAb-SPEs and dAb-Au-NPFe_2O_3NC with peroxidase-like activity	CD63	PLAP	Chronoamperometry (TMB/H_2O_2) "Signal on"	LR: 10^3–10^7 exosomes mL^{-1} LOD: 10^3 exosomes mL^{-1}	Isolation and detection from cell culture media	[72]
AuE	Immunosensor in connection with an aptamer, RCA and HRP-mimicking Hemin/G-Quadruplex	CD63	SGC7901	DPV (H_2O_2) "Signal on"	L.R.: 4.8×10^3–4.8×10^6 particles mL^{-1} LOD: 9.54×10^2 particles mL^{-1}	Spiked human plasma samples	[73]
GEC	Sandwich immunoassays using cAb_{CD81}-MBs and dAb_{CD24} or dAb_{CD230} further labeled with secondary HRP-labeled Abs	CD81, CD24 and CD230	MCF7, MDA-MB-231 and SKBR3	Amperometry (HRP/HQ/H_2O_2) "Signal on"	LOD: 1.94×10^5 exosomes μL^{-1} (CD24) and 1.02×10^6 exosomes μL^{-1} (CD340)	Exosomes isolated from BC patients	[74]
GCE	CAb_{CD63}-MBs, $dAb_{PD\text{-}L1}$-DNA probe and HRCA-mediated disassembly of PVP@HRP@ZIF-8	CD63 and PD-L1	MDA-MB-231, L02	SWV (OPD/H_2O_2) "Signal on"	LR: 1×10^3–1×10^{10} particles mL^{-1} LOD: 334 particles mL^{-1}	Undiluted serum samples from BC patients	[75]
GCE	Immunosensor developed at a Nafion-AuNPs-GCE and using C_{60}–Au-TB composite	EGFR	A549	SWV (TB) "Signal on"	LR: 5×10^4–5×10^9 exosomes mL^{-1} LOD: 2.6×10^4 exosomes mL^{-1}	Spiked human serum	[68]
SPCE	Sandwich immunoassay involving cAb-MBs, b-dAb and Strep-HRP	CD147	SW480, SW620, KM12C, KM12SM, KM12L4a	Amperometry (HRP/HQ/H_2O_2) "Signal on"	LR: 0.096–5.0 ng mL^{-1} (CD147 protein) LOD: 29 pg mL^{-1} (CD147 protein)	Lysed and entire exosomes isolated from CRC cells	[76]
ITO	Tri-channel immunosensor for enzyme-free and label-free detection of multiple exosome biomarkers	CEA, NSE and Cyfra21-1	NCI–H1395, NCI–H226, and NCI–H446	DPV ($[Fe(CN)_6]^{3-/4-}$) "Signal-off"	LR: 10^{-3}–10 ng mL^{-1} (CEA), 10^{-4}–10^2 ng mL^{-1} (NSE), and 10^{-3}–10^2 ng mL^{-1} (Cyfra21-1) LOD: 10^{-4} ng mL^{-1}	Isolated exosomes	[77]
SPGE	Integrated electrochemical biosensor by exploiting the use of ZIF-8 self-assembled on electrodes modified with MB-labeled DNA molecules and an enzyme-base logic system using Suc-Ab_1 and GOx-Ab_2	EpCAM, HER2, PD-L1, miR-21	SK-BR-3, UACC-812, MCF-7, MCF-10A	SWV (MB) "Signal on"	LOD: ~250 vesicles/10 μL sample	Blood samples from BC patients	[78]
ITO	BFC-based self-powered biosensor involving the use of a cAb_{CD63}-AuNPs-ITO and GDH@ZIF-8 in the cathode and $[Fe(CN)_6]^{3-}$/UiO-66]/AuNPs-ITO in the anode	CD63	MCF-7, HL-7702	Cell voltage ($K_3[Fe(CN)_6]$) "Signal on"	LOD: 300 particles mL^{-1}	Spiked FBS	[66]
- Aptasensors/Aptamer-based strategies -							
AuE	Aptamer-MBs in connection with messenger DNAs and Exo III-assisted target recycling amplification	PSMA	LNCaP	DPV ($Ru(NH_3)_6^{3+}$) "Signal off"	LOD: 70 particles μL^{-1}	Spiked FBS	[79]
ITO	Microfluidic platform involving Tim4-MBs and a single-stranded DNA hairpin structure with a G-rich mimicking DNAzyme sequence	CD63	HepG2	DPV (Thi/H_2O_2/NADH) "Signal on"	LR: 7.61×10^4–7.61×10^8 particles mL^{-1} LOD: 4.39×10^3 particles mL^{-1}	Serum from healthy individuals and liver cancer patients	[80]
GCE	Aptasensor based on a DenAu/rGO/GCE, copper (I)-catalyzed click chemistry and HCR	CD63	MCF-7	DPV (HRP/H_2O_2/OPD) "Signal on"	LR: 1.12×10^2–1.12×10^8 particles μL^{-1} LOD: 96 particles μL^{-1}	Exosomes isolated from serum samples from a healthy individual and a BC patient	[64]
DBCO/AuE	Aptamer-MBs in connection with an aptamer and a CTSDR involving MB-probes	CD63	HepG2	SWV (MB) "Signal on"	LR: 1×10^5–5×10^7 particles mL^{-1} LOD: 1.72×10^4 particles mL^{-1}	Spiked human serum samples	[69]
AuE	Aptamer-MBs, Target-Triggered Three-Dimensional DNA Walking Machine and Exonuclease III-assisted ratiometric biosensing strategy in connection with Fc- and MB-DNA probes	EpCAM and CD63	MCF-7, HeLa and HEK-293T	DPV (Fc and MB) "Signal off" (MB) and "Signal on" (Fc)	LR: 5.0×10^4–1.0×10^{10} particles mL^{-1} LOD: 1.3×10^4 particles mL^{-1}	Plasma samples from BC patients	[81]
AuE	Aptasensor based on the use of a CD63-specific aptamer-modified AuE and HRP-pSC_4-AuNPs@COFs nanoprobes	CD63	Colo 205 and NCM-460	Chronoamperometry (HRP/TMB/H_2O_2) "Signal on"	LR: 5×10^2–10^7 particles μL^{-1} LOD: 160 particles μL^{-1}	Human serum from CRC	[82]
GCE		CD63 (aptamer	MCF-7	DPV (MB) "Signal on"		MCF-7 cells-secreted exosomes supplemented	[83]

(*continued on next page*)

Table 2 (*continued*)

Electrode	Rationale	Target biomarker	Target cell/s from which exosomes derive	Electrochemical transduction	Analytical characteristics	Application	Ref.
	$Aptamer_1$-MBs in connection with $aptamer_2$ NA Walker, Ag@C core-shell nanocomposites and a CS-GCE	1) and EpCAM (aptamer 2)			LR: 100−75 000 particles μL^{-1} LOD: 40 particles μL^{-1}	with ultracentrifuged exosomes-free FBS	
AuE	Aptasensor based on the use of and AuE nanostructured with DNA NTHs and AuNPs-DNA conjugates coupled with HRP as labels	CD63	HepG2	Chronoamperometry (H_2O_2/TMB) "Signal on"	LOD: 1.66×10^4 particles mL^{-1}	Plasma samples of a mice with liver cancer in different stages	[84]
AuE	Multipedal DNA walking nanomachine using CD63 aptamer-modified Fe_3O_4@Au NPs and MB-labeled probes	CD63	HeLa	SWV (MB) "Signal off"	LR: 10−2000 exosomes μL^{-1} LOD is 6 exosomes μL^{-1}	Spiked serum samples	[85]
ITO	Dual-signal and intrinsic self-calibration aptasensor based on a MB-labeled-aptamer-BPNSs/Fc/ZIF-67/ITO platform	CD63	MCF-7	SWV (MB and Fc) "Signal off" (MB) "No signal change" (Fc)	LOD: 100 particles mL^{-1}	Spiked serum samples and plasma samples from BC patients	[86]
SPCE	Detachable microfluidic device implemented with an aptasensor involving an aptamer-GNS/NC/SPCE, and an aptamer-AgNPs as detector probes	EpCAM	MCF-7	DPV (AgNPs) "Signal on"	LR: 1×10^2−1×10^9 exosomes μL^{-1} LOD: 17 exosomes μL^{-1}	Samples of BC patients at different stages of the disease	[87]
Micropatterned AuE	Aptasensor using HCR with b-probes and Avi-HRP	CD63 and EpCAM	MCF-7 and PC3	Chronoamperometry (TMB/H_2O_2) "Signal on"	LR: 2.5×10^3−1×10^7 exosomes mL^{-1} LOD: 5×10^2 exosomes mL^{-1}	Serum samples from lung cancer patients	[67]
GCE	Aptamer-PAMAM-AuNPs-GCE and Aptamer-PB-Ti_3C_2 MXene	CD63	HeLa, OVCAR and BT474	SWV (PB) "Signal on"	LR: 5×10^2−5×10^5 particles μL^{-1} LOD: 229 particles μL^{-1}	Spiked serum samples	[88]
SPE	A label-free and enzyme-free approach based on the use of Zr-MOF functionalized paper, aptamer and HCR to generate HRP-mimicking Hemin/G-Quadruplex	CD63	MCF-7	DPV (TMB/H_2O_2) "Signal off"	LR: 1.7×10^4−3.4×10^8 particles mL^{-1} LOD: 5×10^3 particles mL^{-1}	Spiked FBS	[89]
AuE	Electrochemical biosensor exploiting the use of aptamer-MBs, SNAs-based cascade signal amplification and the interaction between cholesterol group and exosomes membrane	EpCAM	MCF-7	SWV (MB) "Signal on"	LR: 1.1×10^2−1.1×10^5 particle μL^{-1} LOD: 44 particles μL^{-1}	Plasma samples from CRC patients	[90]
AuE	Electrochemical aptasensor based on mHCR and interaction between cholesterol group and exosomes membrane	EpCAM	MCF-7	Chronoamperometry (TMB/H_2O_2) "Signal on"	LR: 5×10^2−1×10^5 exosomes μL^{-1} LOD: 285 exosomes μL^{-1}	Serum samples from BC patients	[91]
ITO	Dual-aptamer recognition system based on a cholesterol-modified DNA probe, hyperbranched HCR amplification and ratiometric dual-signal strategies	CD63 and MUC1	MCF-7	DPV ($[Ru(NH_3)_6]^{3+}$ and $[Fe(NH_3)_6]^{3-}$) "Signal off" ($[Ru(NH_3)_6]^{3+}$) "Signal on" ($[Fe(NH_3)_6]^{3-}$)	LOD: 3.0×10^4 particles mL^{-1}	Serum samples from BC patients	[92]
PVDF	Hierarchical Au nanoarray-modified 2D Ti_2CT_x MXene membranes modified with two specific aptamers	EpCAM and CD63	A549	DPV ($[Fe(CN)_6]^{3-/4-}$) "Signal on"	L.R.: 1×10^2−1×10^7 particles μL^{-1} LOD: 58 particles μL^{-1}	Spiked FBS	[70]
- Peptide-based biosensors and biosensing strategies -							
AuE	Label-free peptide-based biosensor in connection with Zr-MOFs encapsulated with MB	EGFR and EGFRvIII	U87	SWV (MB) "Signal on"	LR: 9.5×10^3−1.9×10^7 particles μL^{-1} LOD: 7.83×10^3 particles μL^{-1}	Serum samples from GBM patients	[93]
- ECL detection -							
GCE	Immunosensor based on multivalent PAMAM-AuNPs electrode interface and g-C_3N_4@Galinstan-PDA- nanoprobes	GPC1	HeLa, OVCAR-3 and BT474	ECL (Galinstan NPs and g-C_3N_4 nanosheets) "Signal on"	LR: 50−10^5 particles μL^{-1} LOD: 31 particles μL^{-1}	Spiked serum, urine, and blood samples	[57]
GCE	Aptamer-PNIPAM-AuNPs/GCE and aptamer-modified two-dimensional material Ti_3C_2 MXenes nanosheets as nanoprobes	EpCAM	MCF-7	ECL (luminol, ECL) "Signal on"	LOD: 125 particles μL^{-1}	Spiked serum samples	[94]
GCE	Aptamer/SA-PAM/GCE as scaffolds and AuNPs-MXenes-Aptamer as nanoprobes	CD63	HeLa, OVCAR and HepG2	ECL (luminol) "Signal on"	LR: 10^2−10^5 particles μL^{-1} LOD: 30 particles μL^{-1}	Spiked serum samples	[95]
GCE	Dual mode detection aptasensor using ILs-SiO_2 NUs-GCE as scaffold and MXenes-BPQDs@Ru(dcbpy)$_3^{2+}$-PEI-Ab_{CD63} as nanoprobes	EpCAM and CD63	MCF-7, HeLa	ECL ($Ru(dcbpy)_3^{2+}$) and phototermal "Signal on"	LR: 1.1×10^2−1.1×10^7 particle μL^{-1} LOD: 37 particle μL^{-1}	Spiked human serum	[96]
GCE	Aptasensor implemented at a RuSi NPs-modified GCE coupling to the use of a DNA	CD63	HepG2	ECL (H_2O_2 and $Ru(bpy)_3$		Exosomes extracted from different cell lines	[65]

Table 2 (*continued*)

Electrode	Rationale	Target biomarker	Target cell/s from which exosomes derive	Electrochemical transduction	Analytical characteristics	Application	Ref.
	walking amplification and a GOx labeled DNA probe			$^{2+}$—TPrA system) "Signal off"	LR: 200−75 000 particles μL^{-1} LOD: 60 particles μL^{-1}		
ITO	Aptamer-ITO/NiO/BiOI/Au NP and DNA_2-modified CdSe QDs as nanoprobes	EpCAM	MCF-7, HeLa, HEK-293T	ECL (BiOI/ITO/NiO "Signal on"	LR: 1.0×10^3−1.0×10^8 particles μL^{-1} LOD: 1.2×10^2 particles μL^{-1}	Spiked FBS and exosomes isolated from BC patients	[97]
GCE	4-ABA/GCE modified with CD63 aptamer and MUC1 aptamer-modified Ru@SiO_2 nanoparticles as signaling nanoprobes	MUC1 and CD63	MCF-7, SK-BR-3, and MDA-MB-231	ECL ($Ru(bpy)_3^{2+}$) "Signal on"	LR: 3.22×10^{-4} −156 μg mL^{-1} LOD: 2.73×10^{-4} μg mL^{-1}	Human serum of a BC patient	[98]
GCE	Strategy based on the use of stimuli-responsive DNA microcapsules carrying CdS QDs, a specific aptamer, a DSN-assisted target recycling amplification and a SWCNHs/CS/GCE	EpCAM	MCF-7, HeLa, HepG2 and HEK-293 T	ECL (CdS QDs) "Signal on"	LR: 5×10^4−1×10^8 particles mL^{-1} LOD: 2.1×10^4 particles mL^{-1}	Spiked FBS	[35]
GCE	Sandwich-based biosensor involving the use of PS-specific peptide-AuNFs-GCE and PS-specific peptide-Lum-AuNPs@g-C_3N_4 nanocomposite as signaling probes	PS	SKOV3ip	ECL (luminol/H_2O_2) "Signal on"	LR: 1.0×10^2−1.0×10^7 particles μL^{-1} LOD: 39 particles μL^{-1}	Ovarian cancer cell SKOV3ip exosomes and non-cancerous human peritoneal mesothelial cell HMrSV5 exosomes	[99]

4-ABA: 4-aminobenzoic acid; AuNFs: Au nanoflowers; Au−NPFe_2O_3NC: gold-loaded ferric oxide nanocubes; Avi: avidin; BC: breast cancer; BFCs: biofuel cells; b: biotin; BPQDs: black phosphorous quantum dots; cAb: capture antibody; CEA: carcino-embryonic antigen; CHT: chitosan; DenAu: dendritic gold nanostructure; GPC1: glypican-1; COFs: Covalent organic frameworks; CRC: colorectal cancer; CS: chitosan; CTSDR: cascade toehold-mediated strand displacement reaction; Cyfra21-1: cytokeratin 19 fragments; dAb: detector antibody; DBCO/GE: dibenzocyclooctyne-functionalized gold electrode; DPV: differential pulse voltammetry; DSN: duplex-specific nuclease; ECL: electrogenerated chemiluminescence; EGFR: epidermal growth factor receptor; EGFRvIII: EGFR variant (v) III mutation; EIS: electrochemical impedance spectroscopy; EVs: extracellular vesicles; FBS: fetal bovine serum; Fc: ferrocene; GBM: glioblastoma; GCE: glassy carbon electrode; GDH: glucose dehydrogenase; GEC: graphite epoxy composite; GNP: graphene nanoplatelets; GOx: glucose oxidase; HCR: hybridization chain reaction; HER2: human epidermal growth factor receptor-type2; HRP: horseradish peroxidase; ITO: indium tin oxide; LOD: limit of detection; LR: linear range; MB: methylene blue; MBs: magnetic microbeads; mHCR: multidirectional hybridization chain reaction; MOF: metal−organic framework: NSE: neuron-specific enolase; NTH: nanotetrahedron; OPD: o-phenylenediamine; PAM: poly(acrylamide); PB: prussian blue; PD-L1: programmed death ligand-1; PLAP: placenta alkaline phosphatase; PS: phosphatidylserine; PSMA: prostate-specific membrane antigen; PVDF: polyvinylidene fluoride; PVP@HRP@ZIF-8: pH-responsive protein-encapsulated ZIF-8; QDs: quantum dots; RCA: rolling circle amplification; rGO: reduced graphene oxide; SA: sodium alginate; SiO_2 NUs: SiO_2 nanourchin; SNAs: spherical nucleic acids; SPCE: screen-printed carbon electrode; SPE: screen-printed electrode; SPGE: screen-printed gold electrode; Strep: streptavidin; Suc: sucrase; SWCNHs: single-walled carbon nanohorns; SWV: square wave voltammetry; TB: toluidine blue; TdT: terminal deoxynucleotidyl transferase; Thi: thionine; TMB: 3,3′-5,5′-tetramethylbenzidine.

marker CD63 and the HRP mimicking activity of the hemin/G-quadruplex DNAzyme toward H_2O_2 reduction was exploited for the electrochemical transduction. Another immunosensor was prepared by immobilizing an antibody selective to the EGFR biomarker on a Nafion-AuNPs-GCE via Au−NH_2 bonding that employed the grafted onto the surface of captured exosomes through "carboxyl-Zr^{4+}-phosphate" chemistry of a C_{60}−Au-Toluidine blue (TB) composite and used voltammetry of TB as the redox tracer [68]. Both immunosensors allowed the sensitive determination of gastric [73] and lung cancer cell-derived exosomes [68] and were applied to the analysis of spiked serum samples.

Another interesting strategy is the sandwich immunoassay reported by Cao et al. [75] that cleverly combined the use of CAb_{CD63}-MBs, the $dAb_{PD\text{-}L1}$-DNA probe and an in-situ amplification of hyperbranched rolling circle (HRCA), which lowered the environmental pH leading to the disassembly of pH-responsive protein-encapsulating ZIF-8 (PVP@HRP@ZIF-8) and the release of multiple HRP molecules (Fig. 9a) thus allowing a SWV detection in the presence of *o*-phenylenediamine (OPD)/H_2O_2 at a GCE. In addition to the sensitive determination of PD-$L1^+$ exosomes attributed to the significant amplification achieved by the HRCA (see comparison of curves 2 and 3 in Fig. 9b), the method was successfully applied to the analysis of undiluted serum samples of BC patients and demonstrated the possibility of discrimination between patients with non-metastatic and metastatic BC.

Among the methods using aptamers, those reported by An et al. [64], Cao et al. [69], Zhao et al. [81], Wang et al. [82], Jiang et al. [84], Sun et al. [86], Liu et al. [89] and Wang et al. [90] deserve special mention.

An et al. prepared an electrochemical aptasensor based on click chemistry and HCR for signal amplification. A specific CD63 aptamer was immobilized on a GCE dually nanostructured with reduced graphene oxide and a dendritic gold nanostructure (DenAu/rGO/GCE). The exosomes captured on the immunoplatform were conjugated with alkyne 4-oxo-2-nonenal (alkyne-4-ONE) and further with an azide-labeled DNA probe via a copper(I)-catalyzed click chemistry, that triggered HCR leading to the formation of a long DNA homohybrid carrying multiple biotin molecules which were subsequently labeled with Strep-HRP [64]. Employing DPV in the presence of OPD and H_2O_2, the immunosensor allowed the sensitive determination of exosomes derived from MCF-7 cells and exosomes isolated from serum of a BC patient.

The method reported by Cao et al. used cAb_{CD63}-MBs for the efficient capture of exosomes which were recognized by a catalytic DNA probe containing the aptamer region of CD63 (probe a), that initiated a catalytic molecule machine that relied on the cascade-mediated strand displacement reaction (CTSDR) [69]. The azide/MB duplexes generated as the products of molecule machine were detected by SWV on a dibenzocyclooctyne (DBCO)-modified AuE electrode. This method employed capture and detection bioreceptors of different nature (antibody and aptamer, respectively) although they recognized the same target (CD63). Moreover, the constant recycling of "probe a" led to a significant amplification factor, achieving a LOD of 1.72×10^4 HepG2-derived exosomes mL^{-1} and allowed their analysis in spiked serum samples.

Zhao et al. reported a ratiometric strategy assisted by MBs and

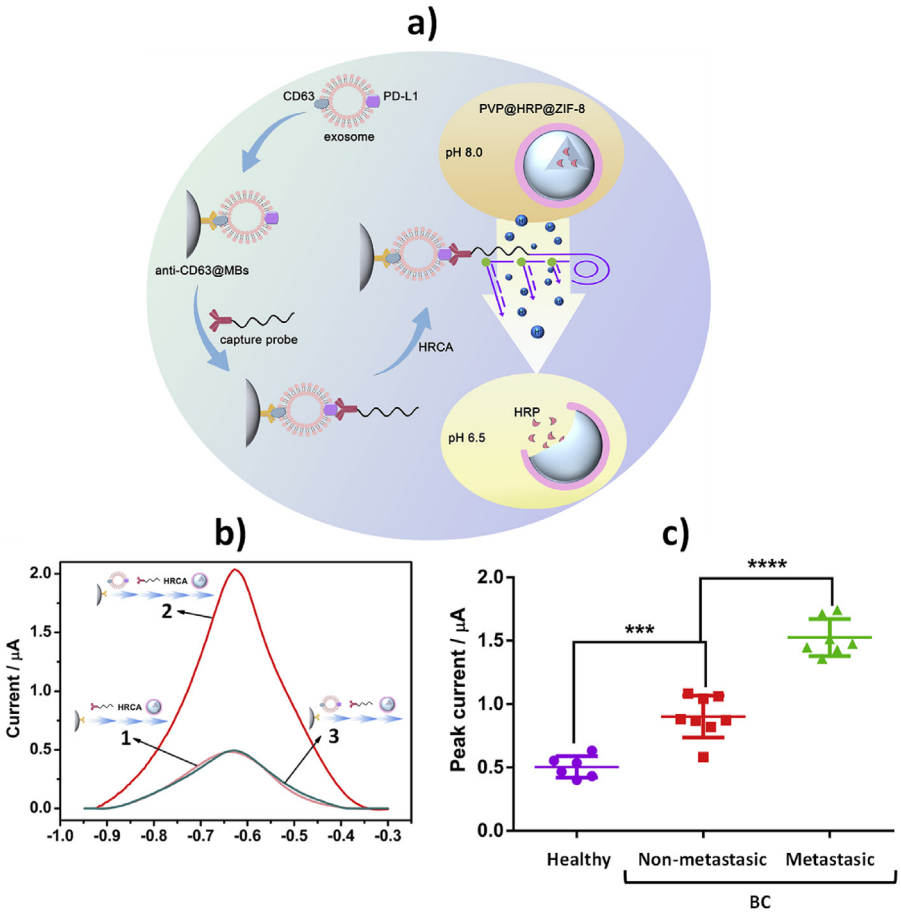

Fig. 9. a) Schematic diagram of the proposed immunoassay for the determination of PD-L1^{+} exosomes combining the use of CAb_{CD63}-MBs, $dAb_{PD\text{-}L1}$-DNA probe and HRCA amplification. b) Electrochemical responses obtained in the absence (1) and the presence (2) of exosomes and in the presence of exosomes but without using HRCA (3). (c) Scatter plots of peak OPD oxidation currents for healthy controls, non-metastatic and metastatic BC patients' serum samples. Reprinted from Ref. [75] with permission, Copyright (2020) Elsevier.

using aptamers specific to CD63 and EpCAM, and amplifications based on target-triggered three-dimensional DNA walking machine and exonuclease III-assisted strategy in connection with ferrocene (Fc)- and methylene blue (MB)-labeled DNA probes [81]. As shown in Fig. 10a, the strategy involved MBs modified with CD63 aptamers and DNAzyme substrates containing a ribonucleobase (rA) cleavage site on each substrate and a swing arm containing one-part EpCAM aptamer and one-part DNAzyme. DNAzyme and its substrate only assemble in the presence of the target exosomes and the Mg^{2+} cofactor triggered the catalytic activity of DNAzyme, leading to cleavage of the substrate at the rA position releasing the oligonucleotide fragments of probe P1 and DNAzyme from the surface of MBs. The free DNAzyme walker was subsequently bound to an adjacent substrate and the process was repeated until all substrates were exhausted. The released P1 strands were then exposed to a MB-labeled hairpin probe-modified AuE, triggering Exo III digestion, which moved the MB molecules away from the electrode surface and recycled the P1 strands. After cyclic shearing, many short strands could be hybridized with the Fc-DNA probes remained on the electrode. Therefore, the presence of exosomes resulted in decreased and increased MB and Fc DPV oxidation peaks, respectively, (Fig. 10b). This method permitted the sensitive determination of MCF-7-derived exosomes and was employed for their determination in plasma samples of BC patients, which (as shown in Fig. 10c) exhibited a significantly larger exosomes concentration than healthy individuals.

An attractive aptasensor using a CD63-specific aptamer-modified AuE through thiol chemistry and spherical covalent organic frameworks (COFs) functionalized with para-sulfocalix [4] arene hydrate (pSC_4)-modified AuNPs and HRP (HRP-pSC_4-AuNPs@COFs) as nanoprobes was reported by Wang et al. for the chronoamperometric detection, in the presence of TMB/H_2O_2, of CRC cell-derived exosomes (Fig. 11) [82]. The method combined the use of pSC_4 as a linker to bind exosomes through various amino acid residues on their surface, AuNPs with excellent conductivity to accelerate the migration of cargo carriers and enhance the aptasensor response, and the high porosity and exoskeleton of COFs which allowed transporting many HRP molecules while maintaining their functionality. The aptasensor achieved a LOD of 160 particles μL^{-1} and was able to distinguish CRC patients from healthy individuals by interrogating target exosomes in serum samples.

Jing et al. reported an aptasensor for the determination of liver cancer-related exosomes by immobilizing an aptamer specific to CD63 on an AuE electrode nanostructured with DNA NTHs and employing AuNPs-DNA conjugates coupled with HRP as nanocarriers of signaling elements for amplification purposes [84]. The aptasensor employed chronoamperometric transduction in the presence of TMB/H_2O_2 and was applied to the analysis of plasma samples of mice with liver cancer in different stages, finding that the concentration of exosomes correlated with tumor size.

A dual-signal, intrinsically self-calibrating aptasensor, that used

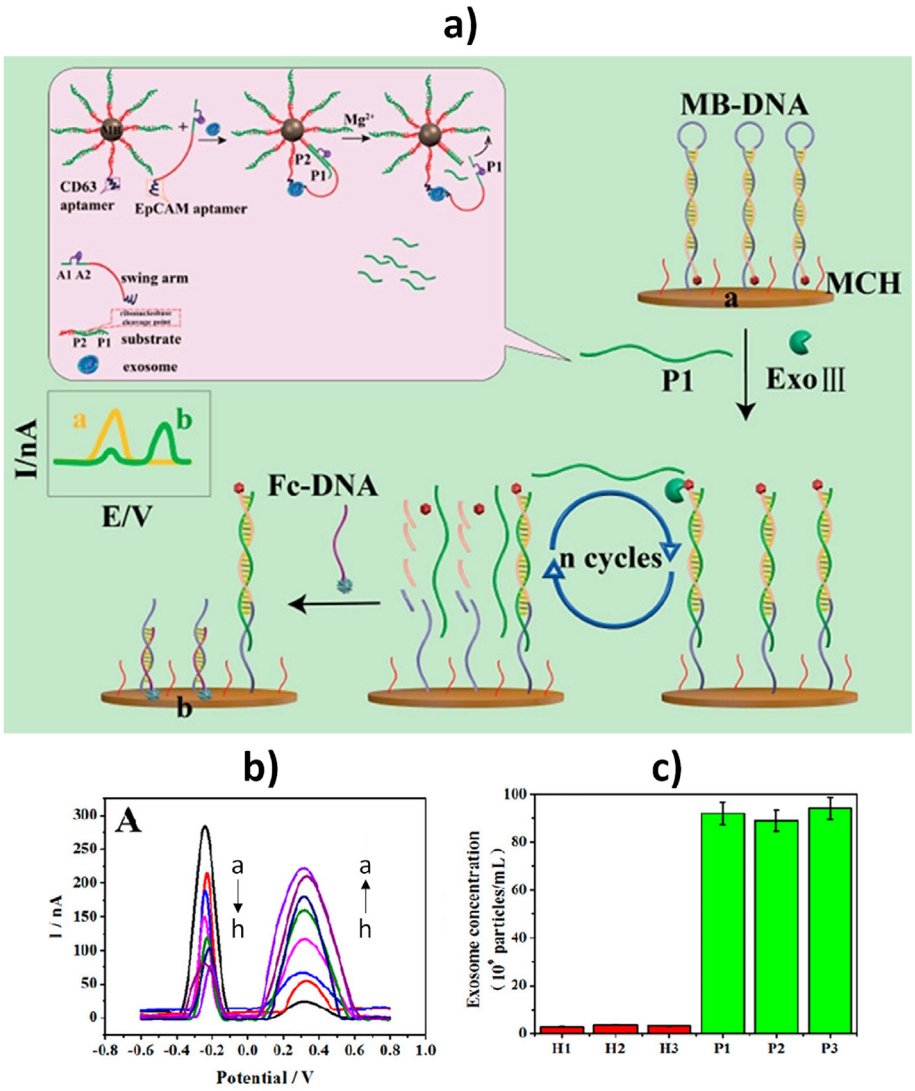

Fig. 10. a) Schematic diagram of a ratiometric method developed for the determination of MCF-7-derived exosomes. The method combined the use of MBs, CD63and EpCAM-specific aptamers and target-triggered three-dimensional DNA walking machine and exonuclease III-assisted amplifications. b) Responses obtained by DPV for different concentrations of exosomes derived from MCF-7 cells (a–h: 0, 5.0×10^4, 1.0×10^5, 1.0×10^6, 1.0×10^7, 1.0×10^8, 1.0×10^9 and 1.0×10^{10} particles mL^{-1}). c) Concentrations of exosomes found in plasma samples from 3 healthy individuals (H1–H3) and 3 BCE patients (P1–P3). Reprinted from Ref. [81] with permission, Copyright (2019) ACS.

a platform constructed by assembling black phosphorus nanosheets (BPNSs) and ferrocene (Fc)-doped metal–organic frameworks (ZIF-67) on an indium tin oxide (ITO) slice, followed by attachment on the same surface of methylene blue (MB)-labeled single-strand DNA aptamer, was reported by Sun et al. for the determination of MCF-7 cell-derived exosomes [86]. The aptamer-BPNSs/Fc/ZIF-67/ITO platform provided dual redox-signal responses of MB and Fc measured by SWV. In accordance with the aptasensor rationale, the MB signal decreased in the presence of the target exosomes while the Fc signal practically did not change which allowed that this latter was used as reference. This led to the development of an intrinsic self-calibration aptasensor which enabled the sensitive detection of the target exosomes (LOD of 100 particles mL^{-1}) and their determination in plasma samples from BC patients.

Liu et al. reported a label-free and enzyme-free approach using Zr-MOF functionalized paper, aptamer, and HCR to generate HRP-mimicking Hemin/G-Quadruplexes [89]. The method involved the capture of exosomes by Zr-MOFs-modified paper through the formation of Zr–O–P bonds and the recognition of CD63 expressed on their membrane by an aptamer that initiated HCR leading to the formation of multiple G-quadruplexes DNAzymes (Fig. 12) displaying high catalytic activity towards 3,3′-5,5′-tetramethylbenzidine (TMB) depletion, monitored by DPV. The method achieved a LOD of 5×10^3 particles mL^{-1} for the determination of exosomes released from MCF-7 cells and was employed for their determination in spiked FBS samples.

An electrochemical biosensor that employed aptamer-MBs, the interaction between the cholesterol group and the exosome membrane, and a spherical nucleic acid (SNA)-based cascade signal amplification, was reported by Wang et al. [90]. SNA is a type of nanomaterial with a small spherical core (<100 nm) functionalized with a dense and highly oriented oligonucleotide. Fig. 13 shows as the SNA-based signal amplification involved two steps: 1) primer strands extended by terminal deoxynucleotidyl transferase (TdT) that act as template strands to continuously degrade probe A by Exo III, and 2) new generated primer strands polymerized by TdT that act again as template strands to incessantly consume probe A. In

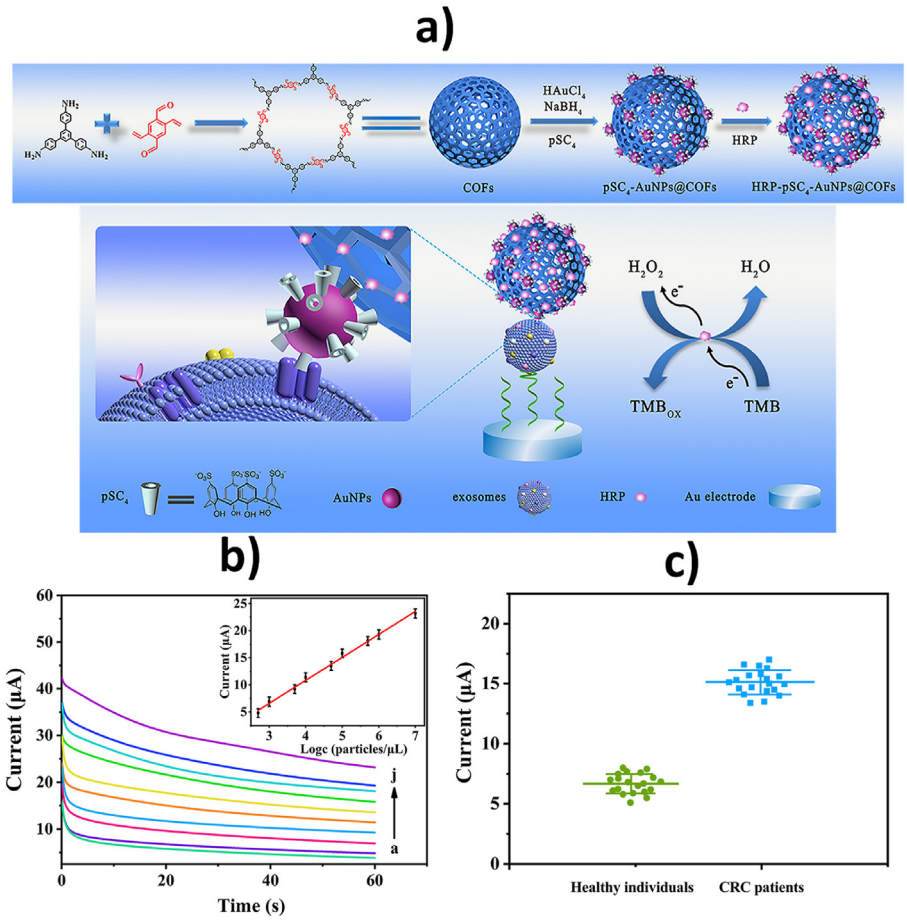

Fig. 11. a) Schematic illustration of the preparation process of HRP-pSC_4-AuNPs@COFs and their use as detector nanoprobes in an aptasensor for the determination of CRC cells-derived exosomes. b) Chronoamperometric responses provided by the aptasensor for different exosome concentrations (a–j: 0, 5×10^2, 10^3, 5×10^3, 10^4, 5×10^4, 10^5, 5×10^5, 10^6 and 10^7 particles μL^{-1}) and the corresponding semi logarithmic calibration as an insert. c) Clinical discrimination using the developed aptasensor for the analysis of the target exosomes in serum samples from healthy individuals and CRC patients. Reprinted from Ref. [82] with permission, Copyright (2020) Elsevier.

the presence of exosomes, captured by CD63-specific aptamer-MBs, primer strands tailored at the 5′ end with a cholesterol group anchored into the exosomes membrane to form SNAs. After magnetic separation, MB-labeled probe A hybridized with extended primer strands of SNAs can be excised by Exo III, producing a truncated probe A with a free 3′-OH group, able to act as a new primer strand to be extended again by TdT. As a result, probe A was endlessly depleted, leading to a decrease in the electrochemical response (oxidation signal of MB monitored by SWV). The achieved triple amplification of this biosensor relies on: 1) one exosome can bind with a number of primer strands; 2) one primer strand of SNAs can be extended by TdT and then act as template strands to digest numerous probe A; 3) truncated probe A as a new primer triggers the circle of the second signal amplification progress. Such amplification allowed a LOD for MCF-7-derived exosomes as low as 44 particles μL^{-1} to be achieved. The biosensor was able to discriminate healthy subjects from CRC patients.

The methodologies using ECL detection are gaining ground due to the inherent advantages of this detection over pure electrochemistry in terms of low background signal, good sensitivity, a wide detection range and a simple optical setup [65].

Illustrative examples are the works reported by Liu's group [63,94,95] using aptamer or immunosensor affinity bioplatforms prepared on GCE electrodes with different modifications: poly(-amidoamine) dendrimer or poly (N-isopropylacrylamide), carboxylic acid terminated coated AuNPs, or with sodium alginate (SA), and poly(acrylamide) (Fig. 14), and using different types of nanoprobes (g-C_3N_4@Galinstan-PDA, aptamer-Ti_3C_2 MXenes nanosheets and AuNPs-MXenes-aptamer). These biosensors were benefited by the unique features inherent to the different types of nanomaterials, used both as electrode modifiers and advanced labels. The resulting methods were applied to the determination of exosomes derived from different types of cancer cells providing LOD values between 30 and 125 particles μL^{-1} and were also applied to supplemented serum samples.

Feng et al. developed an aptasensor implemented at a RuSi NPs-modified GCE coupling the use of a DNA walking machine, which exhibited a strong amplification ability by utilizing the directional autonomous motion of a DNA walking strand to introduce multiple binding signal events, and a glucose oxidase (GOx) labeled DNA probe for the determination of HepG2-derived exosomes [65].

Another interesting method involving stimuli-responsive DNA microcapsules carrying CdS QDs, a specific aptamer, a duplex-specific nuclease (DSN)-assisted target recycling amplification and a GCE modified with single-walled carbon nanohorns (SWCNHs) and chitosan (CS) (Fig. 15) was reported by Guo et al. [35]. The authors interrogated EpCAM in target exosomes and detected the released CdS QDs by ECL.

On the other hand, although modern peptides are experiencing an unstoppable boom in the development of high-performance electrochemical biosensors due to their unique advantages [100], to our knowledge only two biosensors that used these synthetic

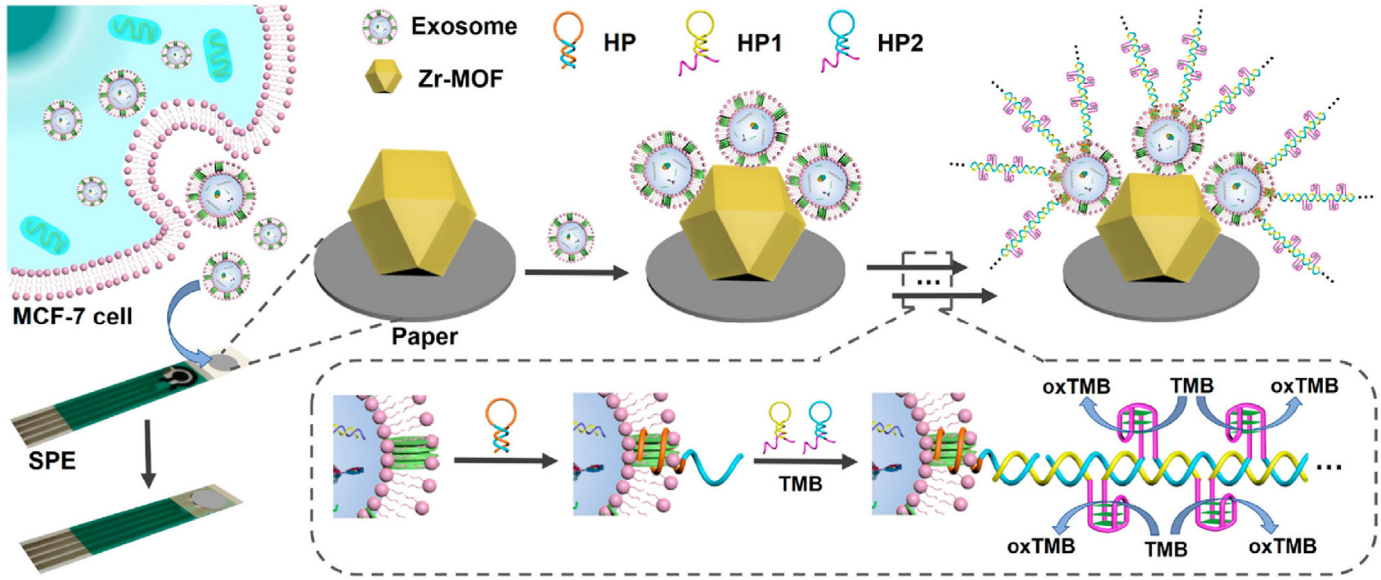

Fig. 12. Principle of the Zr-MOF-functionalized paper-based electrochemical sensor prepared for the label and enzyme-free determination of MCF-7 cells-derived exosomes exploiting HCR to generate multiple HRP-mimicking DNAzymes. Reproduced from Ref. [89] with permission, Copyright (2021) ACS.

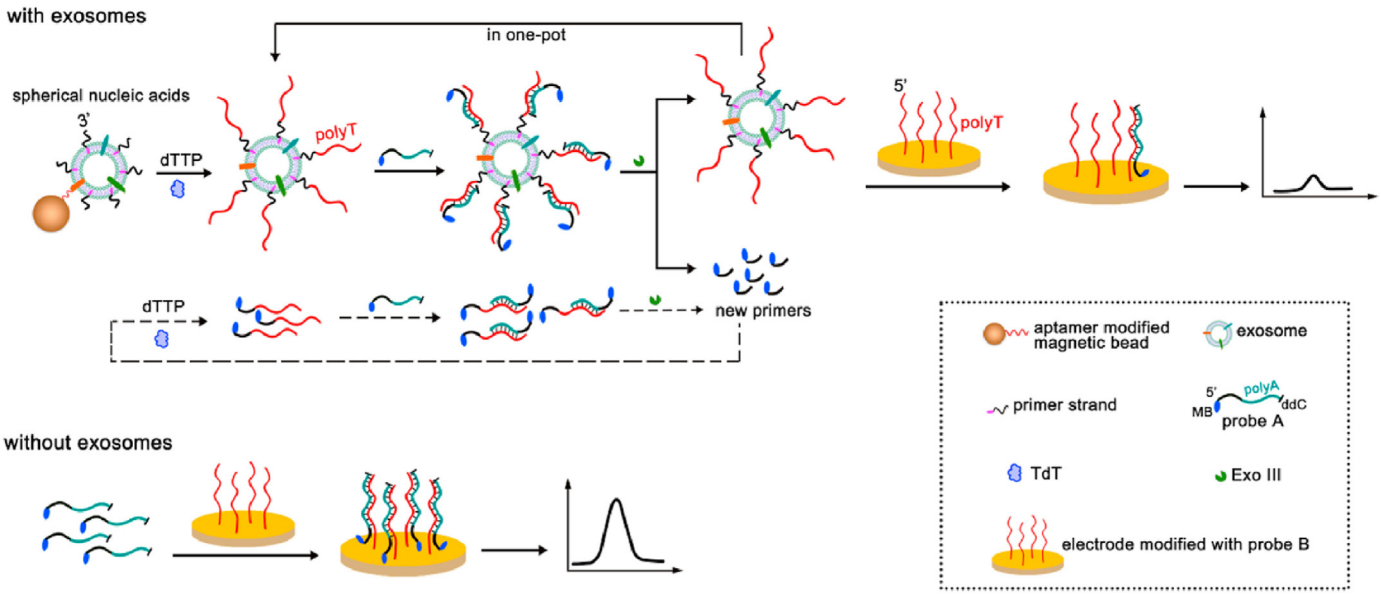

Fig. 13. Rationale of the method involving the selective capture of MCF-7-derived exosomes with aptamer-MBs and their detection using primer strands tailored at the 5′ end with a cholesterol group able to be anchored to the exosomes' membrane, as well as a SNA-based signal amplification. Reprinted from Ref. [90] with permission, Copyright (2021) Elsevier.

bioreceptors have been reported for interrogating exosomes [93,99], employing electrochemical or ECL detection. The label-free biosensor developed by Sun et al. involved the use of an AuE modified with a peptide, by formation of an Au—S bond through the cysteine and the gold surface. The biosensor was able to recognize human epidermal growth factor receptor (EGFR) and EGFR variant (v) III mutation (EGFRvIII), which were overexpressed on the glioblastoma (GBM)-derived exosomes, using Zr-MOFs encapsulated with MB, which were adsorbed on the exosomes surface due to the interaction between Zr^{4+} and the intrinsic phosphate groups outside of exosomes (Fig. 16a) [93]. This peptide biosensor utilized SWV transduction of the MB oxidation response and was applied to the determination of U87-derived exosomes (Fig. 16b), showing ability for early diagnosis and pre and postsurgical monitoring of GBM patients through the analysis of their serum samples (Fig. 16c). The peptide biosensor that used ECL transduction exploited a sandwich format involving a GCE modified with phosphatidylserine (PS)-specific peptide immobilized on Au nanoflowers (AuNFs) and PS-specific peptide-modified g-C_3N_4 nanosheet loaded with luminol capped AuNPs nanocomposite as signaling probe. The biosensors allowed the determination of ovarian cancer cell-derived exosomes with a LOD value of 39 particles μL^{-1}, as well as the discrimination between ovarian cancer cell SKOV3ip exosomes and non-cancerous human peritoneal mesothelial cell HMrSV5 exosomes [99].

Importantly, the tremendous efforts that have been put into the development of electrochemical biosensors for the determination of exosomes has led to their implementation in microfluidic

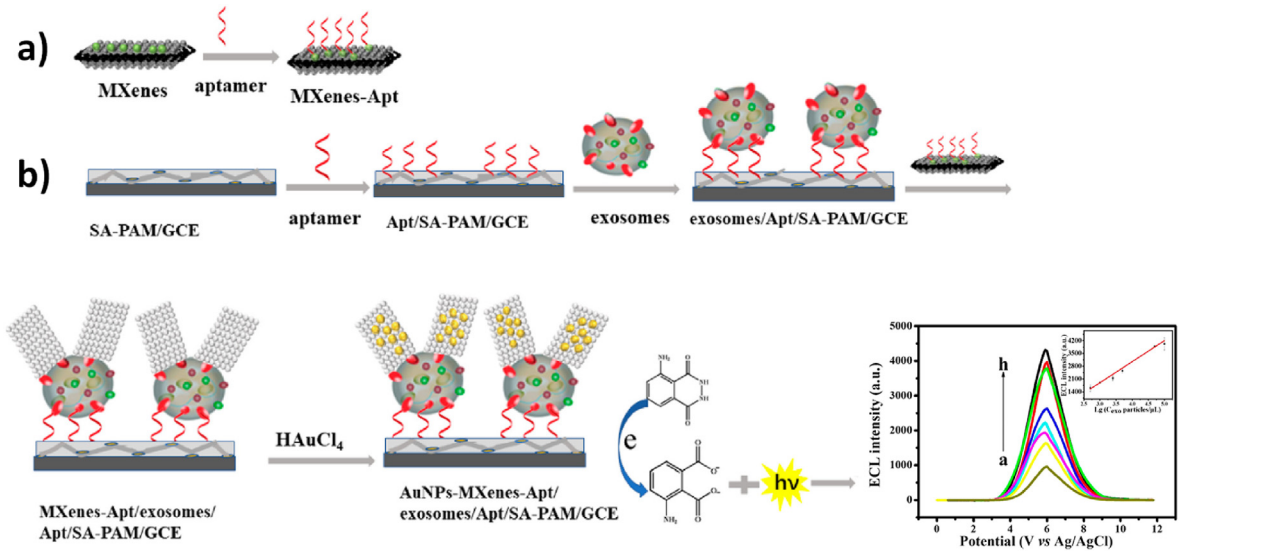

Fig. 14. ECL aptasensor for exosomes released from HeLa cells exploiting the use of an Aptamer/SA-PAM/GCE AuNPs-MXenes-aptamer as nanoprobes. Real ECL intensities obtained for different exosomes concentrations (a–h: 10^2, 5×10^2, 10^3, 2.5×10^3, 5×10^3, 10^4, 5×10^4, 10^5 particles μL^{-1}) are also displayed. Reprinted from Ref. [95] with permission, Copyright (2020) ACS.

devices. Thus, for example, Xu et al. [80] reported a two-stage microfluidic platform integrating on-chip isolation and in situ electrochemical determination of exosomes in blood samples (Fig. 17). The microchip consisted of a Y-shaped micropillar array and a cascaded ITO electrode. The polydimethylsiloxane (PDMS) micropillar array efficiently cross-mixed again and again to increase the collision opportunities between T-cell membrane protein 4 (Tim4)-modified MBs and exosomes (Fig. 17a). The capture of exosomes on MBs occurred through the recognition of the PS expressed in the membranes of exosomes by PS-binding Tim4 receptors in the presence of Ca^{2+}. The captured exosomes were sensitively detected by magnetic enrichment on the surface of an ITO electrode using a single-stranded DNA hairpin structure with a G-rich mimicking DNAzyme sequence caged in the stem-loop structure of the strand. The presence of the target CD63-positive exosomes opened the original single-stranded DNA hairpin and formed a G-quadruplex as a signal reporter which, in the presence of hemin, was employed as the NADH oxidase and HRP-mimicking DNAzyme simultaneously, leading to the continuous catalysis of the newly generated H_2O_2 by NADH oxidation and therefore to a signal enhancement (Fig. 17b). This platform allowed a linear range spanning 5 orders of magnitude and detecting as few as 4.39×10^3 particles mL^{-1} of CD63-positive exosomes in 30 μL of sample and 3.5 h. Furthermore, it was applied to discriminate serum from healthy individuals and liver cancer patients.

More recently, a detachable microfluidic device implemented with an electrochemical aptasensor for highly sensitive and in-situ quantification of MCF-7 derived exosomes was reported [87]. The aptasensor involved the immobilization of an EpCAM-specific aptamer on a SPCE modified with a nanocomposite consisting of MoS_2 nanosheets (MoS_2NS), graphene nanoplatelets (GNP), and chitosan (CS), the recognition of the captured exosomes with an aptamer-AgNPs and the DPV electrochemical detection of the AgNPs oxidation. A microfluidic vortexer to increase the collision between the exosomes and sensing surface using hydrodynamically generated transverse flow was integrated with the aptasensor via a 3D printed magnetic housing. The aptasensor achieved a LOD of 17 exosomes μL^{-1} over a wide dynamic range (1×10^2–1×10^9) exosomes μL^{-1} in a short period and was applied to quantify exosomes in plasma samples of BC patients at different stages of the disease. Moreover, as proof of the concept, the aptasensor could be separated from the 3D printed housing to harvest the exosomes by real-time polymerase chain reaction.

As can be seen, voltammetric techniques have been mainly used for the electrochemical determination of cell-derived exosomes similarly to that happens when targeting whole cells, although EIS, ECL and chronoamperometry have also been employed. Voltammetric techniques such as DPV and SWV, as well as chronoamperometry are not only efficient for the sensitive analysis of different analytes, but also stand out for low-cost equipment, rapid responses, possibility of miniaturization, automation, implementation into continuous analysis and in POC settings and even real-time control in large-scale disease screening. EIS, meanwhile, is considered as a powerful technique with significant application in the analysis of interfacial properties including bio-recognition events (antibody–antigen or substrate–enzyme interactions, nucleic acid and proteins molecular recognition, whole cell capturing, etc.) occurring at the electrode surface. However, EIS is a relatively complex electrochemical technique that needs specialized staff for data interpretation. Moreover, the measurements are not fast, and it is difficult to obtain data at very low frequencies. Regarding ECL, a technique that combines electrochemical and luminescent methods, as it can be seen, it is gaining ground for the monitoring of cancer-related biomarkers due, among other characteristics, to its high selectivity, fast response times, and wide detection ranges. However, it is still in its infancy, both in use and instrumentation, compared to pure electrochemical techniques that have been researched and applied for many more years.

4.3. Cell secretomes

In recent years, the study of cellular secretome is gaining importance in precision diagnosis and therapy. Secretome refers to all the molecules secreted by a cell or shed from its membrane, and it is fundamental for cell-cell communication. Despite the secretome has commonly been defined only by the protein fraction, it also includes non-protein components such as lipids, miRNAs and messenger-RNAs (mRNAs) isolated in or secreted via vesicular bodies [101,102]. Secretome proteins play an important role in many essential physiological and pathophysiological processes,

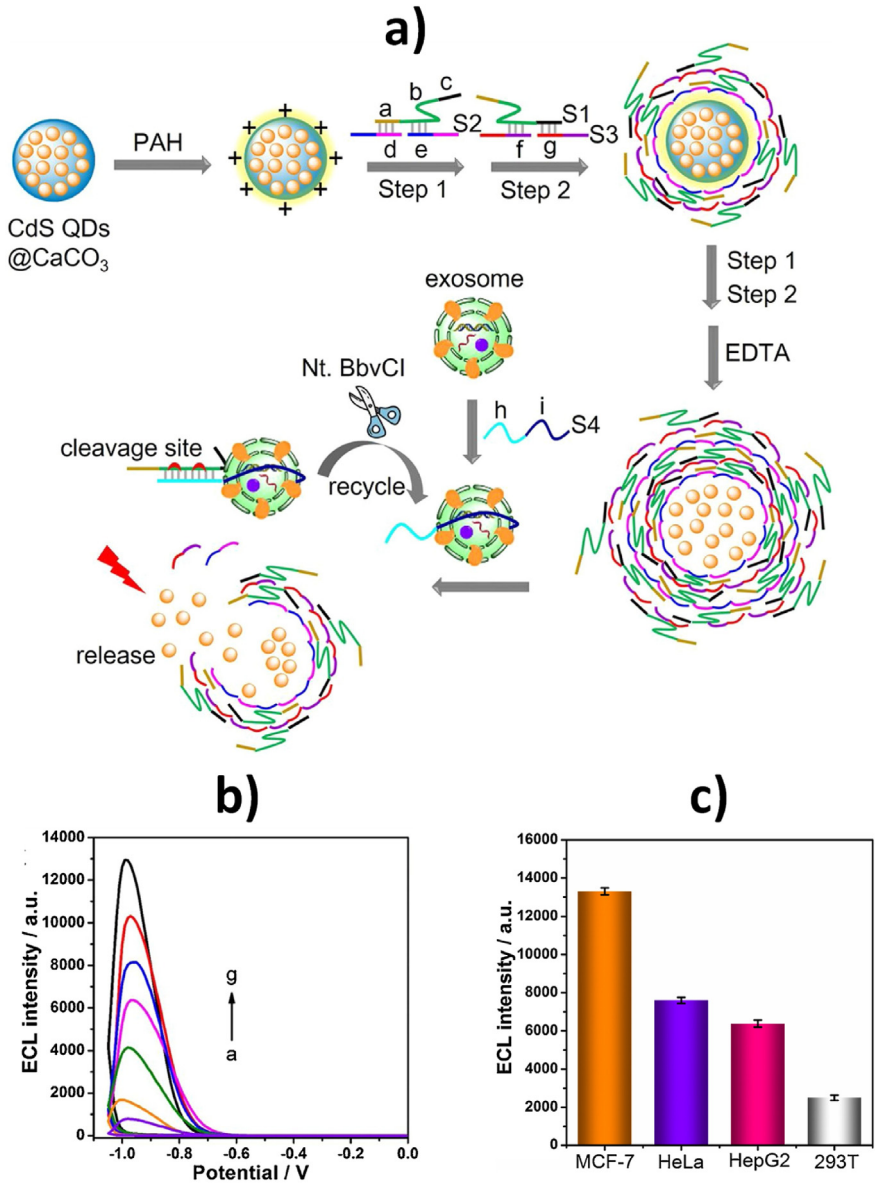

Fig. 15. a) Synthesis of CdS QDs-loaded DNA microcapsules and their coupling with target recycling amplification for homogeneous ECL detection of BC cells-derived exosomes. b) ECL curves obtained for b) increasing exosomes concentration released from MCF-7 cells (a–g: 5×10^4, 1×10^5, 5×10^5, 2×10^6, 5×10^6, 1×10^7, and 1×10^8 particles mL^{-1}) and c) 1×10^8 particles mL^{-1} exosomes extracted from different cancer cells. Reprinted from Ref. [35] with permission, Copyright (2021) Elsevier.

such as cell growth and differentiation, angiogenesis, tumor growth, metastasis, chemoresistance and immune dysregulation [102].

Therefore, the analysis of the cellular secretome, of highly complex nature, is considered of great interest both to shed light on molecular mechanisms and on vital molecules (candidate biomarkers) involved in the progression of relevant diseases.

It is important to note that unlike what happened with the determination of whole cells and exosomes, the applications of electrochemical affinity biosensors for the determination of cellular secretome proteins are very limited and restricted to those by Pingarrón/Campuzano, Barderas and Lobo-Castañón groups for the determination of TFG-β1 [103], GAS6 [104] and total and glycosylated haptoglobin (Hp) fraction [105] in secretomes of pericytes (PCs, mural cells that embrace endothelial cells in capillaries, embedded in the same basement membrane) [103] and CRC cells [103,104].

In all these cases, sandwich immunoassay formats were implemented on the surface of MBs and used labeling with the HRP enzyme and amperometric transduction on SPCEs trough the H_2O_2/HQ system. It is important to highlight that it was not possible to performe these determinations by conventional ELISA methodologies due to lack of sensitivity, and that in the case of TFG-β1 analysis on PCs secretomes, they contributed to demonstrate the role of PCs in the tumor microenvironment. According to the obtained results, TGF-β mediated crosstalk between PCs and CRC cells (HCT116) modulated PC secretome and the high levels they expressed of TGF-β1 were responsible for initiating an autocrine activation loop that caused IGFBP-3 release, which in turn is a key paracrine factor in triggering migration and invasion of CRC cells [103].

Regarding the works on GAS6 and Hp, the results obtained in the determination of secretomes of CRC cells with different metastatic potential, allowed correlating the response provided by the

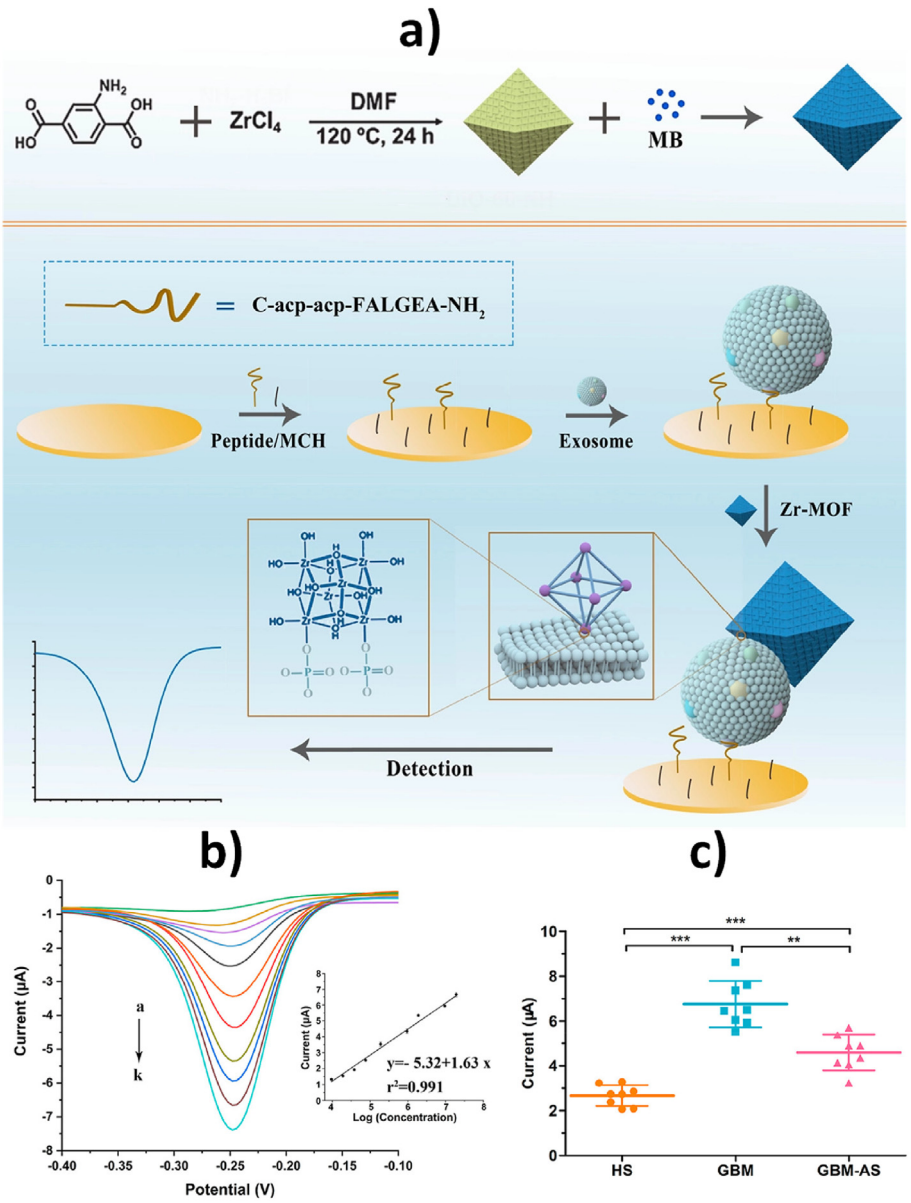

Fig. 16. (a) Schematic diagram of the preparation of the MB@UiO-66-based nanoprobes and the resulting electrochemical biosensor for the determination of GBM-derived exosomes. (b) SWV response recorded for different concentrations of exosomes (a–k: 0, 9.5×10^3, 1.9×10^4, 3.8×10^4, 7.6×10^4, 1.9×10^5, 9.5×10^5, 1.9×10^6, 9.5×10^6, 1.9×10^7 and 9.5×10^7 particles μL^{-1}) and inset of the semi logarithmic linear range obtained. (c) Scatter plots of exosomes obtained for serum samples of healthy individuals (HS) and GBM patients without surgery (GBM), and after surgery (GBM-AS). Reprinted from Ref. [93] with permission, Copyright (2020) ACS.

bioplatform for the analyzed marker (GAS6) with the tumorigenic and metastatic potential of each cell [104] and what is more relevant to quantify in a simple and simultaneous way, using a quadruple bioplatform (Fig. 18), the content of total or glycosylated Hp in undiluted secretomes in only 75 min [105]. Importantly, this electrochemical affinity bioplatform allowed the expressed secretome discrimination of homologous cancer cells with different invasive/metastatic potential, which is highly important to understand their different molecular mechanism of invasion and metastasis.

5. Concluding remarks and perspectives

To date, early detection of prevalent diseases such as cancer has relied on costly, tedious and invasive techniques such as scans and examinations, accompanied by analysis of solid tissue biopsies. Thus, minimally invasive analysis of circulating biomarkers, including the cells and their secretomes and exosomes, with potential for early and individualized diagnosis offers enormous life-saving potential, especially if combined with technologies such as those based on electrochemical biosensing whose great appeal lies in their simple handling, affordable cost and application at the POC or in resource-limited settings. All this would improve life expectancy and quality of life and significantly reduce the cost of managing millions of patients worldwide who could even painlessly and privately self-examine.

As it has been discussed in this critical overview article both generally and individually, biosensing and electrochemical biosensors have experienced incredible advances in recent years and currently are good allies to reinvent and implement precision medicine through the determination of the biomarkers that are flourishing in the state-of-the-art clinic, such as cells, and the

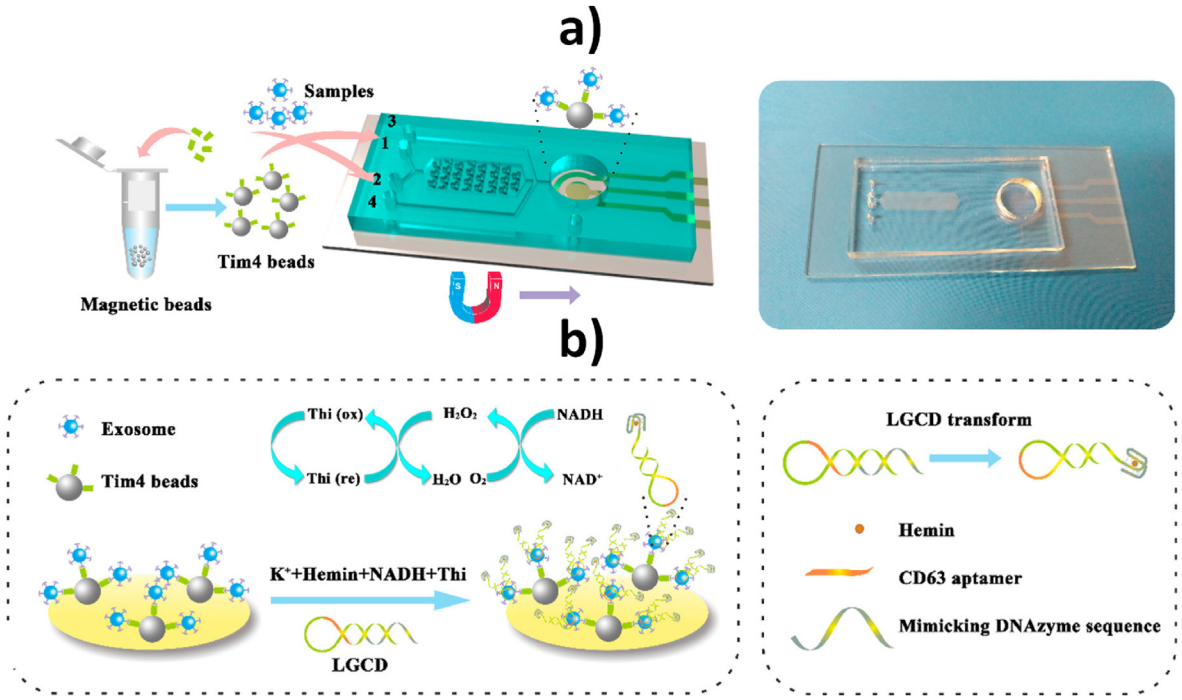

Fig. 17. a) MBs-based microfluidic device for on-chip isolation and detection of tumor-derived exosomes and actual photograph of the chip. b) Schematic diagram of the electrochemical detection process on the ITO electrode. Reproduced from Ref. [80] with permission, Copyright (2018) ACS.

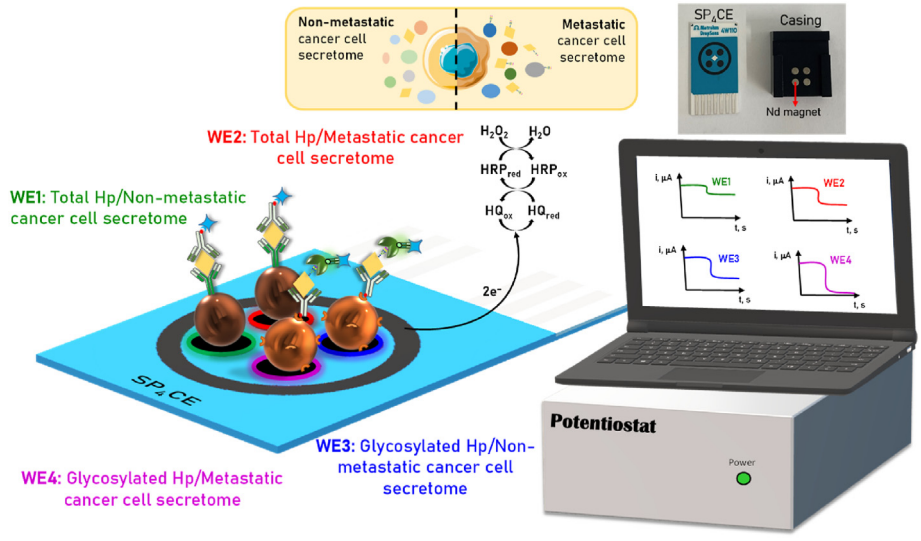

Fig. 18. Schematic diagram of the quadruple bioplatform set up for the simultaneous amperometric determination of total and glycosylated Hp in metastatic and non-metastatic CRC cells secretomes. Reproduced from Ref. [105] with permission, Copyright (2023) Springer.

secretomes and exosomes they release. These advances, which have gone hand in hand with the production, development and application of new electrochemical substrates, attractive surface chemistries, bioassay formats and amplification strategies (either of the target or of the electrochemical response), and new (nano) materials and bioreceptors, have led to the development of superb devices compatible with the high selectivity and sensitivity required for the determination of cells, exosomes and secretomes and capable of pioneering applications of great relevance.

Despite the remarkable progress experienced and the advantages already demonstrated by these biodevices in the determination of cells and exosomes and in the incipient incursion into the analysis of secretomes, in terms of simplicity, versatility, affordability, minimal sample treatment and multiplexed and/or multiomics usefulness even at the point of care, there are still formidable challenges that electrochemical bioplatforms need to be overcome and which, in our opinion, coincide with the main limitations that could be pointed out for these devices. For example, the selectivity and stability of involved nanomaterials and bioreceptors (which can undergo digestion processes) in complex samples must be improved by resorting, for example, to protective biocompatible polymers or multifunctional biomaterials. In terms of applicability, although in the case of exosomes the applications have gone a little further by facing on numerous occasions patient

samples, this is more complex in the case of whole cells due to the high sensitivity required, where, in general, research is still confined to the proof-of-concept stage. Comprehensive clinical validations remain as an unsolved task, which must be faced with sufficient consistency to withstand the onslaught that will be launched by the clinical diagnostics industry. On the other hand, the translation of laboratory research into clinical practice must involve the development of standardized technical specifications, including the collection and handling of biological samples. We must also be aware that the acceptance of these technologies by all the actors involved in the clinical routine is not an easy task either, because it is an extremely conservative and stressed environment, users who are already accustomed to employing other methodologies for the determination of these targets and the interpretation of the data derived from them.

As scientists, increasingly convinced of the versatility and potential of these biodevices, the best we can do is to continue to ask more and more of these devices, to dare to confront them with real samples, with multiplexed and/or multiomics determinations (due to the heterogeneity of cells and exosomes) and to implement them in integrated POC devices which combine multiple separation, isolation, and detection technologies to minimize operator manipulation and the likelihood of introducing error and contamination. Thus, for example, the combination of tumor circulome (circulating tumor DNA, ctDNA, and CTCs), secretome and needle biopsy analysis would allow further study and anticipation of complex processes such as transit and metastatic organotropism and the determination of characteristic biomarkers both outside and inside cells and exosomes especially at the single particle level that would yield valuable information on cell identity and distinctive features. These goals, because of the versatility and unique opportunities afforded by electrochemical biosensing devices, appear to be more difficult than unattainable and are certainly worth including on the to-do list. The use of bioreceptors towards even more specific targets, of bioinspired multivalent or multifunctional probes or the combination of several of them, would allow boosting the recognition efficiency for target cells and exosomes improving specificity. We must also join forces to transfer and take advantage as soon as possible of the achievements made in the field of medical oncology to other clinical fields of interest, such as the diagnosis of other types of prevalent diseases that threaten us, such as neurodegenerative ones, where the same benefits are to be expected. Biosensing and electrochemical biosensors should also unfold their potential in the determination of organoids and in organ-on-chip technologies, fronts that will undoubtedly provide a decisive boost to precision medicine. As it is occurring with electrochemical affinity biosensing of other circulating biomarkers [106], the future will also involve the exploration of other types of substrates such as paper and flexible substrates, in order to one day also being able to provide information regarding these cell biomarkers in real time and in a truly non-invasive way through wireless networking capabilities directly to our smartphones and other mobile devices.

It is indisputable that electrochemical biosensing is making it possible to take important steps to contribute to boosting research and advancing precision medicine, particularly important at this time due to the COVID-19 pandemic, Brexit, the invasion of Ukraine and the rising inflation, but also that there is still a great deal to be done. However, the conviction of all the good that precision diagnostics can offer us at both the personal and societal level and the capabilities of electrochemical biosensing to achieve it, together with collective and constant efforts in allied fields, such as new materials and fabrication technologies and clinical diagnosis, also witnesses to constant innovations, is the ideal breeding ground for the development of new technologies, to continue to witness increasingly important advances in this field and to trust that perhaps we or our descendants will be able to benefit from a precision, equal and accessible diagnosis. This in addition to being a right, will guarantee us a better and longer life, giving us the option of adopting a more active role in our self-care.

Author contributions

Writing—review and editing, SC, MG, MP and JMP; funding acquisition, SC. All authors have read and agreed to the published version of the manuscript.

Declaration of competing interest

The authors declare that they have no known competing financial interests or personal relationships that could have appeared to influence the work reported in this paper.

Data availability

No data was used for the research described in the article.

Acknowledgements

The financial support of PID2019-103899RB-I00 (Spanish Ministerio de Ciencia e Innovación) and TRANSNANOAVANSENS-CM Program from the Comunidad de Madrid (S2018/NMT-4349) are gratefully acknowledged.

References

[1] T.D. Pollard, J.J. Ong, A. Goyanes, M. Orlu, S. Gaisford, M. Elbadawi, A.W. Basit, Electrochemical biosensors: a nexus for precision medicine, Drug Discov. Today 26 (1) (2021) 69–79. https://doi.org/10.1016/j.drudis.2020.10.021.
[2] P. Pinzani, V. D'Argenio, M. Del Re, C. Pellegrini, F. Cucchiara, F. Salvianti, S. Galbiati, Updates on liquid biopsy: current trends and future perspectives for clinical application in solid tumors, Clin. Chem. Lab. Med. 59 (7) (2021) 1181–1200. https://doi.org/10.1515/cclm-2020-1685.
[3] S. Singh, P.S. Podder, M. Russo, C. Henry, S. Cinti, Tailored point-of-care biosensors for liquid biopsy in the field of oncology, Lab Chip 23 (2023) 44–61. https://doi.org/10.1039/d2lc00666a.
[4] S.H. Gawel, L. Jackson, N. Jeanblanc, G.J. Davis, Current and future opportunities for liquid biopsy of circulating biomarkers to aid in early cancer detection, J. Cancer Metastasis Treat 8 (2022) 26. https://doi.org/10.20517/2394- 4722.2022.13.
[5] M.R. Hasan, M.S. Ahommed, M. Daizy, M.S. Bacchu, M.R. Ali, M.R. Al-Mamun, M. Aly Saad Aly, M.Z.H. Khan, S.I. Hossain, Recent development in electrochemical biosensors for cancer biomarkers detection, Biosens. Bioelectron. X 8 (2021), 100075. https://doi.org/10.1016/j.biosx.2021.100075.
[6] R. Lorenzo-Gómez, R. Miranda-Castro, N. de-los-Santos-Álvarez, M.J. Lobo-Castañón, Electrochemical aptamer-based assays coupled to isothermal nucleic acid amplification techniques: new tools for cancer diagnosis, Curr. Opin. Electrochem. 14 (2019) 32–43. https://doi.org/10.1016/j.coelec.2018.11.008.
[7] X. Ma, Y. Hao, L. Liu, Progress in nanomaterials based optical and electrochemical methods for the assays of exosomes, Int. J. Nanomed. 16 (2021) 7575–7608. https://doi.org/10.2147/IJN.S333969.
[8] X.-X. Peng, X. Qin, Y. Qin, Y. Xiang, G.-J. Zhang, F. Yang, Bioprobes-regulated precision biosensing of exosomes: from the nanovesicle surface to the inside, Coord. Chem. Rev. 463 (2022), 214538. https://doi.org/10.1016/j.ccr.2022.214538.
[9] D. Sun, J. Lu, L. Zhang, Z. Chen, Aptamer-based electrochemical cytosensors for tumor cell detection in cancer diagnosis: a review, Anal. Chim. Acta 1082 (2019) 1–17. https://doi.org/10.1016/j.aca.2019.07.054.
[10] Z. Zhang, Q. Li, X. Du, M. Liu, Application of electrochemical biosensors in tumor cell Detection, Thorac. Cancer 11 (2020) 840–850. https://doi.org/10.1111/1759-7714.13353.
[11] I.R. Suhito, K.-M. Koo, T.-H. Kim, Recent advances in electrochemical sensors for the detection of biomolecules and whole cells, Biomedicines 9 (2021) 15. https://doi.org/10.3390/biomedicines9010015.
[12] R. Ziółkowski, M. Jarczewska, Ł. Górski, E. Malinowska, From small molecules toward whole cells detection: application of electrochemical aptasensors in modern medical diagnostics, Sensors 21 (2021) 724. https://doi.org/10.3390/s21030724.
[13] W. Lattanzi, C. Ripoli, V. Greco, M. Barba, F. Iavarone, A. Minucci, A. Urbani,

C. Grassi, O. Parolini, Basic and preclinical research for personalized medicine, J. Personalized Med. 11 (2021) 354. https://doi.org/10.3390/jpm11050354.
[14] European Groundshot—addressing Europe's cancer research challenges: a *Lancet Oncology* Commission. www.thelancet.com/oncology Published online November 15, 2022. https://doi.org/10.1016/S1470-2045(22)00540-X.
[15] P. Krzyszczyk, A. Acevedo, E.J. Davidoff, L.M. Timmins, I. Marrero-Berrios, M. Patel, C. White, C. Lowe, J.J. Sherba, C. Hartmanshenn, K.M. O'Neill, M.L. Balter, Z.R. Fritz, I.P. Androulakis, R.S. Schloss, M.L. Yarmush, The growing role of precision and personalized medicine for cancer treatment, Technology, Singap World Sci) 6 (3–4) (2018) 79. https://doi.org/10.1142/S2339547818300020.
[16] H. Hampel, A. Vergallo, G. Perry, S. Lista, Alzheimer precision medicine initiative (APMI). The alzheimer precision medicine initiative, J. Alzheimers Dis. 68 (2019) 1. https://doi.org/10.3233/JAD-181121.
[17] M. Labib, S.O. Kelley, Circulating tumor cell profiling for precision oncology, Mol. Oncol. 15 (2021) 1622–1646. https://doi.org/10.1002/1878-0261.12901.
[18] V. Rodrigues da Costa, R. Pinheiro Araldi, H. Vigerelli, F. D'Ámelio, T.B. Mendes, V. Gonzaga, B. Policíquio, G.A. Colozza-Gama, C.W. Valverde, I. Kerkis, Exosomes in the tumor microenvironment: from biology to clinical applications, Cells 10 (10) (2021) 2617. https://doi.org/10.3390/cells10090000.
[19] M.-Z. Jin, R.-R. Han, G.-Z. Qiu, X.-C. Ju, G. Lou, W.-L. Jin, Organoids, An intermediate modeling platform in precision oncology, Cancer Lett. 414 (2018) 174–180. https://doi.org/10.1016/j.canlet.2017.11.021.
[20] Y. Li, P. Tang, S. Cai, J. Peng, G. Hua, Organoid based personalized medicine: from bench to bedside, Cell Regen. 9 (2020) 21. https://doi.org/10.1186/s13619-020-00059-z.
[21] L. Shariati, Y. Esmaeili, S.H. Javanmard, E. Bidram, A. Amini, Organoid technology: current standing and future perspectives, Stem Cell. 39 (12) (2021) 1625–1649. https://doi.org/10.1002/stem.3379.
[22] M. Oliveira, P. Conceição, K. Kant, A. Ainla, L. Diéguez, Electrochemical sensing in 3D cell culture models: new tools for developing better cancer diagnostics and treatments, Cancers 13 (2021) 1381. https://doi.org/10.3390/cancers13061381.
[23] M. Jung, S. Ghamrawi, E.Y. Du, J.J. Gooding, M. Kavallaris, Advances in 3D bioprinting for cancer biology and precision medicine: from matrix design to application, Adv. Healthcare Mater. 11 (2022), 2200690. https://doi.org/10.1002/adhm.202200690.
[24] S. Campuzano, R. Barderas, P. Yáñez-Sedeño, J.M. Pingarrón, Electrochemical biosensing to assist multiomics analysis in precision medicine, Curr. Opin. Electrochem. 28 (2021), 100703. https://doi.org/10.1016/j.coelec.2021.100703.
[25] S.S. Spring, S. Goggins, C.G. Frost, Ratiometric electrochemistry: improving the robustness, reproducibility and reliability of biosensors, Molecules 26 (2021) 2130. https://doi.org/10.3390/molecules26082130.
[26] P. Yáñez-Sedeño, A. González-Cortés, S. Campuzano, J.M. Pingarrón, Copper(I)-catalyzed click chemistry as a tool for the functionalization of nanomaterials and the preparation of electrochemical (bio)sensors, Sensors 19 (2019) 2379. https://doi.org/10.3390/s19102379.
[27] S. Campuzano, F. Kuralay, M.J. Lobo-Castañón, M. Bartošík, K. Vyavahare, E. Paleček, D.A. Haake, J. Wang, Ternary monolayers as DNA recognition interfaces for direct and sensitive electrochemical detection in untreated clinical samples, Biosens. Bioelectron. 26 (2011) 3577–3583. https://doi.org/10.1016/j.bios.2011.02.004.
[28] V. Ruiz-Valdepeñas Montiel, J.R. Sempionatto, B. Esteban-Fernández de Ávila, A. Whitworth, S. Campuzano, J.M. Pingarrón, J. Wang, Delayed sensor activation based on transient coatings: biofouling protection in complex biofluids, J. Am. Chem. Soc. 140 (2018) 14050–14053. https://doi.org/10.1021/jacs.8b08894.
[29] S. Campuzano, M. Pedrero, P. Yáñez-Sedeño, J.M. Pingarrón, Antifouling (bio) materials for electrochemical (bio)sensing, Int. J. Mol. Sci. 20 (2019) 423. https://doi.org/10.3390/ijms20020423.
[30] S. Campuzano, M. Pedrero, P. Yáñez-Sedeño, J.M. Pingarrón, Nanozymes in electrochemical affinity biosensing, Microchim. Acta 187 (2020) 423. https://doi.org/10.1007/s00604-020-04390-9.
[31] R. Bruch, M. Johnston, A. Kling, T. Mattmüller, J. Baaske, S. Partel, S. Madlener, W. Weber, G.A. Urban, C. Dincer, CRISPR-powered electrochemical microfluidic multiplexed biosensor for target amplification-free miRNA diagnostics, Biosens. Bioelectron. 177 (2021), 112887. https://doi.org/10.1016/j.bios.2020.112887.
[32] Q.A. Phan, L.B. Truong, D. Medina-Cruz, C. Dincer, E. Mostafavi, CRISPR/Cas-powered nanobiosensors for diagnostics, Biosens. Bioelectron. 197 (2022), 113732. https://doi.org/10.1016/j.bios.2021.113732.
[33] M. Deng, F. Li, X. Zuo, M. Li, CRISPR/Cas-powered biosensing, Analy. Sen. 3 (2023), e202200052. https://doi.org/10.1002/anse.202200052.
[34] H. Peng, Z. Huang, W. Wu, M. Liu, K. Huang, Y. Yang, H. Deng, X. Xia, W. Chen, Versatile high-performance electrochemiluminescence ELISA platform based on a gold nanocluster probe, ACS Appl. Mater. Interfaces 11 (27) (2019) 24812–24819. https://doi.org/10.1021/acsami.9b08819.
[35] Y. Guo, Q. Cao, C. Zhao, Q. Feng, Stimuli-responsive DNA microcapsules for homogeneous electrochemiluminescence sensing of tumor exosomes, Sensor. Actuator. B Chem. 329 (2021), 129136. https://doi.org/10.1016/j.snb.2020.129136.
[36] Y. Cao, Y. Dai, H. Chen, Y. Tang, X. Chen, Y. Wang, J. Zhao, X. Zhu, Integration of fluorescence imaging and electrochemical biosensing for both qualitative location and quantitative detection of cancer cells, Biosens. Bioelectron. 130 (2019) 132–138. https://doi.org/10.1016/j.bios.2019.01.024.
[37] D. Sun, J. Lu, D. Chen, Y. Jiang, Z. Wang, W. Qin, Y. Yu, Z. Chen, Y. Zhang, Label-free electrochemical detection of HepG2 tumor cells with a self-assembled DNA nanostructure-based aptasensor, Sensor. Actuator. B Chem. 268 (2018) 359–367. https://doi.org/10.1016/j.snb.2018.04.142.
[38] X. Wu, T. Xiao, Z. Luo, R. He, Y. Cao, Z. Guo, W. Zhang, Y. Chen, A micro-/nano-chip and quantum dots-based 3D cytosensor for quantitative analysis of circulating tumor cells, J. Nanobiotechnol. 16 (2018) 65. https://doi.org/10.1186/s12951-018-0390-x.
[39] S. Tang, H. Shen, Y. Hao, Z. Huang, Y. Tao, Y. Peng, Y. Guo, G. Xie, W. Feng, A novel cytosensor based on Pt@Ag nanoflowers and AuNPs/Acetylene black for ultrasensitive and highly specific detection of circulating tumor cells, Biosens. Bioelectron. 104 (2018) 72–78. https://doi.org/10.1016/j.bios.2018.01.001.
[40] N. Soda, K. Clack, M.J.A. Shiddiky, Recent advances in liquid biopsy technologies for cancer biomarker detection, Sens. Diagn. 1 (2022) 343. https://doi.org/10.1039/d2sd00010e.
[41] J.-X. Liu, N. Bao, X. Luo, S.-N. Ding, Nonenzymatic amperometric aptamer cytosensor for ultrasensitive detection of circulating tumor cells and dynamic evaluation of cell surface N-glycan expression, ACS Omega 3 (2018) 8595–8604. https://doi.org/10.1021/acsomega.8b01072.
[42] S.-S. Wang, X.-P. Zhao, F.-F. Liu, M.R. Younis, X.-H. Xia, C. Wang, Direct plasmon-enhanced electrochemistry for enabling ultrasensitive and label-free detection of circulating tumor cells in blood, Anal. Chem. 91 (2019) 4413–4420. https://doi.org/10.1021/acs.analchem.8b04908.
[43] J. Luo, D. Liang, D. Zhao, M. Yang, Photoelectrochemical detection of circulating tumor cells based on aptamer conjugated Cu_2O as signal probe, Biosens. Bioelectron. 151 (2020), 111976. https://doi.org/10.1016/j.bios.2019.111976.
[44] M.E. Fiori, L. Villanova R. De Maria, Cancer stem cells: at the forefront of personalized medicine and immunotherapy, Curr. Opin. Pharmacol. 35 (2011) 1–11. https://doi.org/10.1016/j.coph.2017.04.006.
[45] L. Walcher, A.-K. Kistenmacher, H. Suo, R. Kitte, S. Dluczek, A. Strauß, A.-R. Blaudszun, T. Yevsa, S. Fricke, U. Kossatz-Boehlert, Cancer stem cells—origins and biomarkers: perspectives for targeted personalized therapies, Front. Immunol. 11 (2020) 1280. https://doi.org/10.1016/10.3389/fimmu.2020.01280.
[46] C. Gu, P. Gai, X. Liu, J. Liu, F. Li, Ultrasensitive and versatile homogeneous electrochemical cytosensing platform based on target-induced displacement reaction for "signal-on" bioassay, Sensor. Actuator. B Chem. 270 (2018) 1–8. https://doi.org/10.1016/j.snb.2018.04.167.
[47] L. Bábelová, M.E. Sohová, A. Poturnayová, M. Buríková, J. Bizík, T. Hianik, Label-free electrochemical aptasensor for Jurkat cells detection as a potential diagnostic tool for leukemia, Electroanalysis 30 (2018) 1487–1495. https://doi.org/10.1002/elan.201800091.
[48] D. Chen, D. Sun, Z. Wang, W. Qin, L. Chen, L. Zhou, Y. Zhang, A DNA nanostructured aptasensor for the sensitive electrochemical detection of HepG2 cells based on multibranched hybridization chain reaction amplification strategy, Biosens. Bioelectron. 117 (2018) 416–421. https://doi.org/10.1016/j.bios.2018.06.041.
[49] L. Farzin, M. Shamsipur, L. Samandari, S. Sheibani, Signalling probe displacement electrochemical aptasensor for malignant cell surface nucleolin as a breast cancer biomarker based on gold nanoparticle decorated hydroxyapatite nanorods and silver nanoparticle labels, Microchim. Acta. 185 (2018) 154. https://doi.org/10.1007/s00604-018-2700-2.
[50] D. Sun, J. Lu, Z. Luo, L. Zhang, P. Liu, Z. Chen, Competitive electrochemical platform for ultrasensitive cytosensing of liver cancer cells by using nano-tetrahedra structure with rolling circle amplification, Biosens. Bioelectron. 120 (2018) 8–14. https://doi.org/10.1016/j.bios.2018.08.002.
[51] L. Tian, J. Qi, K. Qian, O. Oderinde, Q. Liu, C. Yao, W. Song, Y. Wang, Copper (II) oxide nanozyme based electrochemical cytosensor for high sensitive detection of circulating tumor cells in breast cancer, J. Electroanal. Chem. 812 (2018) 1–9. https://doi.org/10.1016/j.jelechem.2017.12.012.
[52] M.A. Tabrizi, M. Shamsipur, R. Saber, S. Sarkar, Isolation of HL-60 cancer cells from the human serum sample using MnO_2-PEI/Ni/Au/aptamer as a novel nanomotor and electrochemical determination of thereof by aptamer/gold nanoparticles-poly(3,4-ethylene dioxythiophene) modified GC electrode, Biosens. Bioelectron. 110 (2018) 141–146. https://doi.org/10.1016/j.bios.2018.03.034.
[53] Y. Yang, Y. Fu, H. Su, L. Mao, M. Chen, Sensitive detection of MCF-7 human breast cancer cells by using a novel DNA-labeled sandwich electrochemical biosensor, Biosens. Bioelectron. 122 (2018) 175–182. https://doi.org/10.1016/j.bios.2018.09.062.
[54] S. Yazdanparast, A. Benvidi, M. Banaei, H. Nikukar, M.D. Tezerjani, M. Azimzadeh, Dual-aptamer based electrochemical sandwich biosensor for MCF-7 human breast cancer cells using silver nanoparticle labels and a poly(glutamic acid)/MWNT nanocomposite, Microchim. Acta. 185 (2018) 405. https://doi.org/10.1007/s00604-018-2918-z.
[55] Y. Zhang, S. Luo, B. Situ, Z. Chai, B. Li, J. Liu, L. Zheng, A novel electrochemical cytosensor for selective and highly sensitive detection of cancer cells using binding-induced dual catalytic hairpin assembly, Biosens. Bioelectron. 102 (2018) 568–573. https://doi.org/10.1016/j.bios.2017.12.010.

[56] J. Zhao, Y. Tang, Y. Cao, T. Chen, X. Chen, X. Mao, Y. Yin, G. Chen, Amplified electrochemical detection of surface biomarker in breast cancer stem cell using self-assembled supramolecular nanocomposites, Electrochim. Acta 283 (2018) 1072–1078. https://doi.org/10.1016/j.electacta.2018.07.002.
[57] J. Zhang, H. Chen, Y. Cao, C. Feng, X. Zhu, G. Li, Design nanoprobe based on its binding with amino acid residues on cell surface and its application to electrochemical analysis of cells, Anal. Chem. 91 (2019) 1005–1010. https://doi.org/10.1021/acs.analchem.8b04247.
[58] X. Zhou, Y. Li, H. Wu, W. Huang, H. Ju, S. Ding, A amperometric immunosensor for sensitive detection of circulating tumor cells using a tyramide signal amplification-based signal enhancement system, Biosens. Bioelectron. 130 (2019) 88–94. https://doi.org/10.1016/j.bios.2019.01.023.
[59] Y. Zheng, X. Wang, S. He, Z. Gao, Y. Di, K. Lu, K. Li, J. Wang, Aptamer-DNA concatamer-quantum dots based electrochemical biosensing strategy for green and ultrasensitive detection of tumor cells via mercury-free anodic stripping voltammetry, Biosens. Bioelectron. 126 (2019) 261–268. https://doi.org/10.1016/j.bios.2018.09.076.
[60] M. Freitas, H.P.A. Nouws, E. Keating, C. Delerue-Matos, High-performance electrochemical immunomagnetic assay for breast cancer analysis, Sensor. Actuator. B Chem. 308 (2020), 127667. https://doi.org/10.1016/j.snb.2020.127667.
[61] H. Yang, Y. Zhang, L. Zhang, K. Cui, S. Ge, J. Huang, J. Yu, Stackable Lab-on-paper device with all-in-one Au electrode for high-efficiency photoelectrochemical cyto-sensing, Anal. Chem. 90 (2018) 7212–7220. https://doi.org/10.1021/acs.analchem.8b00153.
[62] S. Campuzano, M. Pedrero, R. Barderas, J.M. Pingarrón, Empowering electrochemical biosensing through nanostructured or multifunctional nucleic acid or peptide biomaterials, Adv. Mater. Technol. 7 (2022), 2200310. https://doi.org/10.1002/admt.202200310.
[63] Y. Zhang, F. Wang, H. Zhang, H. Wang, Y. Liu, Multivalency interface and g-C_3N_4 coated liquid metal nanoprobe signal amplification for sensitive electrogenerated chemiluminescence detection of exosomes and their surface proteins, Anal. Chem. 91 (2019) 12100–12107. https://doi.org/10.1021/acs.analchem.9b03427.
[64] Y. An, T. Jin, Y. Zhu, F. Zhang, P. He, An ultrasensitive electrochemical aptasensor for the determination of tumor exosomes based on click chemistry, Biosens. Bioelectron. 142 (2019), 111503. https://doi.org/10.1016/j.bios.2019.111503.
[65] Q.-M. Feng, P. Ma, Q. Hang Cao, Y.-H. Guo, J.-J. Xu, An aptamer-binding DNA walking machine for sensitive electrochemiluminescence detection of tumor exosomes, Chem. Commun. 56 (2020) 269–272. https://doi.org/10.1039/C9CC08051A.
[66] C. Gu, L. Bai, L. Pu, P. Gai, F. Li, Highly sensitive and stable self-powered biosensing for exosomes based on dual metal-organic frameworks nanocarriers, Biosens. Bioelectron. 176 (2021), 112907. https://doi.org/10.1016/j.bios.2020.112907.
[67] W. Zhang, Z. Tian, S. Yang, J. Rich, S. Zhao, M. Klingeborn, P.-H. Huang, Z. Li, A. Stout, Q. Murphy, E. Patz, S. Zhang, G. Liu, T.J. Huang, Electrochemical micro-aptasensors for exosome detection based on hybridization chain reaction amplification, Microsyst. Nanoeng. 7 (2021) 63. https://doi.org/10.1038/s41378-021-00293-8.
[68] Z. Liu, H. Wang, J. Li, M. Wang, H. Yang, F. Si, J. Kong, Detection of exosomes via an electrochemical biosensor based on C_{60}-Au-Tb composite, Microchem. J. 170 (2021), 106772. https://doi.org/10.1016/j.microc.2021.106772.
[69] Y. Cao, L. Li, B. Han, Y. Wang, Y. Dai, J. Zhao, A catalytic molecule machine-driven biosensing method for amplified electrochemical detection of exosomes, Biosens. Bioelectron. 141 (2019), 111397. https://doi.org/10.1016/j.bios.2019.111397.
[70] Q. You, L. Zhuang, Z. Chang, M. Ge, Q. Mei, L. Yang, W.-F. Dong, Hierarchical Au nanoarrays functionalized 2D Ti_2CT_x MXene membranes for the detection of exosomes isolated from human lung carcinoma cells, Biosens. Bioelectron. 216 (2022), 114647. https://doi.org/10.1016/j.bios.2022.114647.
[71] T. Kilic, A.T. De Sousa Valinhas, I. Wall, P. Renaud, S. Carrara, Label-free detection of hypoxia-induced extracellular vesicle secretion from MCF-7 cells, Sci. Rep. 8 (2018) 9402. https://doi.org/10.1038/s41598-018-27203-9.
[72] K. Boriachek, M.K. Masud, C. Palma, H.-P. Phan, Y. Yamauchi, S.A. Hossain, N.-T. Nguyen, C. Salomon, M.J.A. Shiddiky, Avoiding pre-isolation step in exosome analysis: direct isolation and sensitive detection of exosomes using gold-loaded nanoporous ferric oxide nanozymes, Anal. Chem. 91 (2019) 3827–3834. https://doi.org/10.1021/acs.analchem.8b03619.
[73] R. Huang, L. He, Y. Xia, H. Xu, C. Liu, H. Xie, S. Wang, L. Peng, Y. Liu, Y. Liu, N. He, Z. Li, A sensitive aptasensor based on a Hemin/G-Quadruplex-assisted signal amplification strategy for electrochemical detection of gastric cancer exosomes, Small 15 (2019), 1900735. https://doi.org/10.1002/smll.201900735.
[74] S. Lima Moura, C. García Martín, M. Martí, M.I. Pividori, Electrochemical immunosensing of nanovesicles as biomarkers for breast cancer, Biosens. Bioelectron. 150 (2020), 111882. https://doi.org/10.1016/j.bios.2019.111882.
[75] Y. Cao, Y. Wang, X. Yu, X. Jiang, G. Li, J. Zhao, Identification of programmed death ligand-1 positive exosomes in breast cancer based on DNA amplification-responsive metal-organic frameworks, Biosens. Bioelectron. 166 (2020), 112452. https://doi.org/10.1016/j.bios.2020.112452.
[76] V. Pérez-Ginés, R.M. Torrente-Rodríguez, A. Montero-Calle, G. Solís-Fernández, P. Atance-Gómez, M. Pedrero, José M. Pingarrón, R. Barderas, S. Campuzano, Tackling CD147 exosome-based cell-cell signaling by electrochemical biosensing for early colorectal cancer detection, Biosens. Bioelectron. X 11 (2022), 100192. https://doi.org/10.1016/j.biosx.2022.100192.
[77] C. Fan, B. Jiang, W. Shi, D. Chen, M. Zhou, Tri-Channel electrochemical immunobiosensor for combined detections of multiple exosome biomarkers of lung cancer, Biosensors 12 (2022) 435. https://doi.org/10.3390/bios12070435.
[78] F. Wang, Y. Gui, W. Liu, C. Li, Y. Yang, Precise molecular profiling of circulating exosomes using a Metal–Organic Framework-based sensing interface and an enzyme-based electrochemical logic platform, Anal. Chem. 94 (2022) 875–883. https://doi.org/10.1021/acs.analchem.1c03644.
[79] H. Dong, H. Chen, J. Jiang, H. Zhang, C. Cai, Q. Shen, Highly sensitive electrochemical detection of tumor exosomes based on aptamer recognition-induced multi-DNA release and cyclic enzymatic amplification, Anal. Chem. 90 (2018) 4507–4513. https://doi.org/10.1021/acs.analchem.7b04863.
[80] H. Xu, C. Liao, P. Zuo, Z. Liu, B.-C. Ye, Magnetic-based microfluidic device for on-chip isolation and detection of tumor-derived exosome, Anal. Chem. 90 (2018) 13451–13458. https://doi.org/10.1021/acs.analchem.8b03272.
[81] L. Zhao, R. Sun, P. He, X. Zhang, Ultrasensitive detection of exosomes by target-triggered three-dimensional DNA walking machine and Exonuclease III-assisted electrochemical ratiometric biosensing, Anal. Chem. 91 (2019) 14773–14779. https://doi.org/10.1021/acs.analchem.9b04282.
[82] M. Wang, Y. Pan, S. Wu, Z. Sun, L. Wang, J. Yang, Y. Yin, G. Li, Detection of colorectal cancer-derived exosomes based on covalent organic frameworks, Biosens. Bioelectron. 169 (2020), 112638. https://doi.org/10.1016/j.bios.2020.112638.
[83] Y. Guo, Q. Cao, Q. Feng, Catalytic hairpin assembly-triggered DNA walker for electrochemical sensing of tumor exosomes sensitized with Ag@C core-shell nanocomposites, Anal. Chim. Acta. 1135 (2020) 55–63. https://doi.org/10.1016/j.aca.2020.08.036.
[84] J. Jiang, Y. Yu, H. Zhang, C. Cai, Electrochemical aptasensor for exosomal proteins profiling based on DNA nanotetrahedron coupled with enzymatic signal amplification, Anal. Chim. Acta. 1130 (2020) 1–9. https://doi.org/10.1016/j.aca.2020.07.012.
[85] P. Miao, Y. Tang, A multipedal DNA walker for amplified detection of tumor exosomes, Chem. Commun. 56 (2020) 4982. https://doi.org/10.1039/d0cc01817a.
[86] Y. Sun, H. Jin, X. Jiang, R. Gui, Assembly of black phosphorus nanosheets and MOF to form functional hybrid thin-film for precise protein capture, Dual-signal and intrinsic self-calibration sensing of specific cancer-derived exosomes, Anal. Chem. 92 (2020) 2866–2875. https://doi.org/10.1021/acs.analchem.9b05583.
[87] L. Kashefi-Kheyrabadi, J. Kim, S. Chakravarty, S. Park, H. Gwak, S.-I. Kim, M. Mohammadniaei, M.-H. Lee, K.-A. Hyun, H.-I. Jung, Detachable microfluidic device implemented with electrochemical aptasensor (DeMEA) for sequential analysis of cancerous exosomes, Biosens. Bioelectron. 169 (2020), 112622. https://doi.org/10.1016/j.bios.2020.112622.
[88] H. Zhang, Z. Wang, F. Wang, Y. Zhang, H. Wang, Y. Liu, Ti_3C_2 MXene mediated Prussian blue in situ hybridization and electrochemical signal amplification for the detection of exosomes, Talanta 224 (2021), 121879. https://doi.org/10.1016/j.talanta.2020.121879.
[89] X. Liu, X. Gao, L. Yang, Y. Zhao, F. Li, Metal–Organic Framework-functionalized paper-based electrochemical biosensor for ultrasensitive exosome assay, Anal. Chem. 93 (2021) 11792–11799. https://doi.org/10.1021/acs.analchem.1c02286.
[90] L. Wang, Y. Deng, J. Wei, Y. Huang, Z. Wang, G. Li, Spherical nucleic acids-based cascade signal amplification for highly sensitive detection of exosomes, Biosens. Bioelectron. 191 (2021), 113465. https://doi.org/10.1016/j.bios.2021.113465.
[91] L. Wang, L. Zeng, Y. Wang, T. Chen, W. Chen, G. Chen, C. Li, J. Chen, Electrochemical aptasensor based on multidirectional hybridization chain reaction for detection of tumorous exosomes, Sensor. Actuator. B Chem. 332 (2021), 129471. https://doi.org/10.1016/j.snb.2021.129471.
[92] L. Yang, X. Yin, B. An, F. Li, Precise capture and direct quantification of tumor exosomes via a highly efficient dual-aptamer recognition-assisted ratiometric immobilization-free electrochemical strategy, Anal. Chem. 93 (2021) 1709–1716. https://doi.org/10.1021/acs.analchem.0c04308.
[93] Z. Sun, L. Wang, S. Wu, Y. Pan, Y. Dong, S. Zhu, J. Yang, Y. Yin, G. Li, An electrochemical biosensor designed by using Zr-based Metal–Organic Frameworks for the detection of glioblastoma-derived exosomes with practical application, Anal. Chem. 92 (2020) 3819–3826. https://doi.org/10.1021/acs.analchem.9b05241.
[94] H. Zhang, Z. Wang, Q. Zhang, F. Wang, Y. Liu, Ti_3C_2 MXenes nanosheets catalyzed highly efficient electrogenerated chemiluminescence biosensor for the detection of exosomes, Biosens. Bioelectron. 124–125 (2019) 184–190. https://doi.org/10.1016/j.bios.2018.10.016.
[95] H. Zhang, Z. Wang, F. Wang, Y. Zhang, H. Wang, Y. Liu, In situ formation of gold nanoparticles decorated Ti_3C_2 MXenes nanoprobe for highly sensitive electrogenerated chemiluminescence detection of exosomes and their surface proteins, Anal. Chem. 92 (2020) 5546–5553. https://doi.org/10.1021/acs.analchem.0c00469.
[96] D. Fan, D. Zhao, S. Zhang, Y. Huang, H. Dai, Y. Lin, Black phosphorus quantum dots functionalized MXenes as the enhanced dual-mode probe for exosomes sensing, Sensor. Actuator. B Chem. 305 (2020), 127544. https://doi.org/10.1016/j.snb.2019.127544.

[97] Y. Pei, Y. Ge, X. Zhang, Y. Li, Cathodic photoelectrochemical aptasensor based on NiO/BiOI/AuNP composite sensitized with CdSe for determination of exosomes, Microchim. Acta 51 (2021) 188. https://doi.org/10.1007/s00604-021-04716-1.

[98] R. Li, Y. An, T. Jin, F. Zhang, P. He, Detection of MUC1 protein on tumor cells and their derived exosomes for breast cancer surveillance with an electrochemiluminescence aptasensor, J. Electroanal. Chem. 882 (2021), 115011. https://doi.org/10.1016/j.jelechem.2021.115011.

[99] X. Liu, Q. Wang, J. Chen, X. Chen, W. Yang, Ultrasensitive electrochemiluminescence biosensor for the detection of tumor exosomes based on peptide recognition and luminol-AuNPs@g-C_3N_4 nanoprobe signal amplification, Talanta 221 (2021), 121379. https://doi.org/10.1016/j.talanta.2020.121379.

[100] L. Yuan, L. Liu, Peptide-based electrochemical biosensing, Sensor. Actuator. B Chem. 344 (2021), 130232. https://doi.org/10.1016/j.snb.2021.130232.

[101] D. Capece, D. Verzella, A. Tessitore, E. Alesse, C. Capalbo, F. Zazzeroni, Cancer secretome and inflammation: the bright and the dark sides of NF-κB, Semin. Cell Dev. Biol. 78 (2018) 51–61. https://doi.org/10.1016/j.semcdb.2017.08.004.

[102] J. López de Andrés, C. Griñán-Lisón, G. Jiménez, J.A. Marchal, Cancer stem cell secretome in the tumor microenvironment: a key point for an effective personalized cancer treatment, J. Hematol. Oncol. 13 (2020) 136. https://doi.org/10.1186/s13045-020-00966-3.

[103] R. Navarro, A. Tapia-Galisteo, L. Martín-García, C. Tarín, C. Corbacho, G. Gómez-López, E. Sánchez-Tirado, S. Campuzano, A. González-Cortés, P. Yáñez-Sedeño, M. Compte, L. Álvarez-Vallina, L. Sanz, TGF-β-induced IGFBP-3 is a key paracrine factor from activated pericytes that promotes colorectal cancer cell migration and invasion, Mol. Oncol. 14 (2020) 2609–2628. https://doi.org/10.1002/1878-0261.12779.

[104] C. Muñoz-San Martín, V. Pérez-Ginés, R.M. Torrente-Rodríguez, M. Gamella, G. Solís-Fernández, A. Montero-Calle, M. Pedrero, V. Serafín, N. Martínez-Bosch, P. Navarro, P. García de Frutos, M. Batlle, R. Barderas, J.M. Pingarrón, S. Campuzano, Electrochemical immunosensing of Growth arrest-specific 6 in human plasma and tumor cell secretomes, Electrochem. Sci. Adv. 2 (2022), e2100096. https://doi.org/10.1002/elsa.202100096.

[105] C. Muñoz-San Martín, A. Montero-Calle, M. Garranzo-Asensio, M. Gamella, V. Pérez-Ginés, M. Pedrero, J.M. Pingarrón, R. Barderas, N. de-los-Santos-Alvarez, M.J. Lobo-Castanón, S. Campuzano, First bioelectronic immunoplatform for quantitative secretomic analysis of total and metastasis-driven glycosylated haptoglobin, Anal. Bioanal. Chem. 415 (11) (2023) 2045–2057. https://doi.org/10.1007/s00216-022-04397-6.

[106] S. Campuzano, M. Pedrero, R.M. Torrente-Rodríguez, J.M. Pingarrón, Affinity-based Wearable Electrochemical Biosensors: Natural versus Biomimetic Receptors, Analysis & Sensing, 2022, e202200087. https://doi.org/10.1002/ansе.202200087. In press.